

Neutrino-induced pion production

R. González-Jiménez (UGent),
Wroclaw, Dec 2017

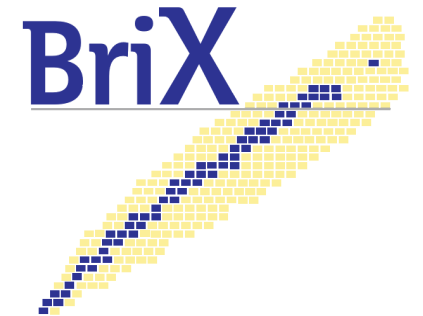


Neutrino-induced pion production



Raúl González Jiménez

Department of Physics and Astronomy,
Ghent University, Belgium



*NuWro Workshop, 3-5 Dec 2017,
Wrocław, Poland*

In collaboration with...

Natalie Jachowicz

Kajetan Niewczas

Jannes Nys

Vishvas Pandey

Tom Van Cuyck

Nils Van Dessel

Outline

I Kinematics

II 1π production on the nucleon

III 1π production off the nucleus

IV Conclusions

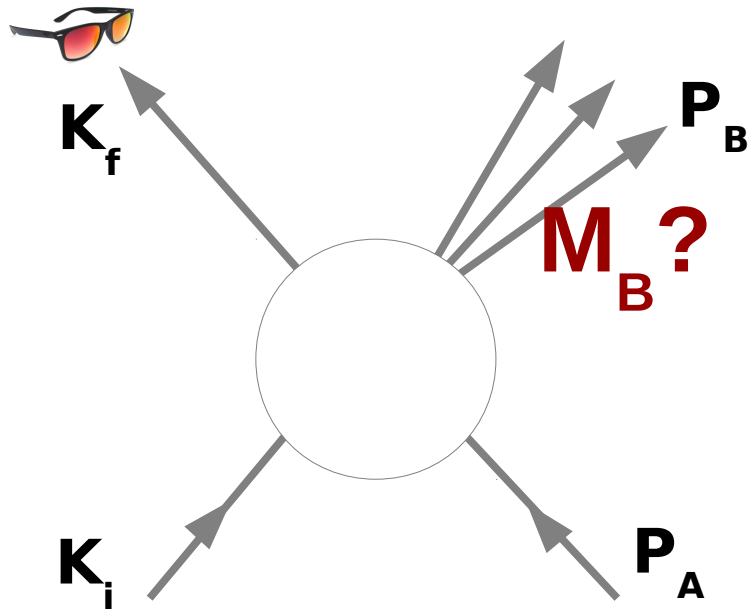
Kinematics

For more check:

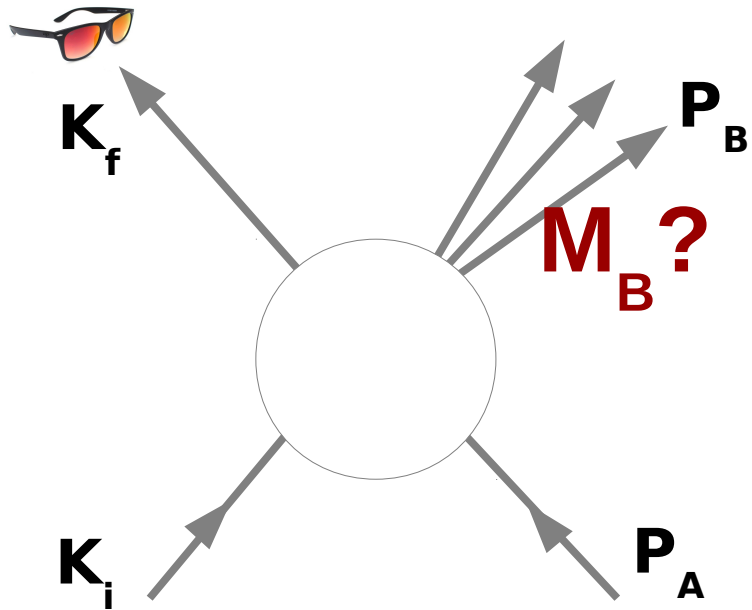
Donnelly, Prog. Part. Nucl. Phys. 13, 183-236 (1985)

Van Orden, Donnelly, Moreno, arXiv:1707.04121

Inclusive scattering on a target at rest: only scattered lepton is detected and we know nothing about final hadronic system



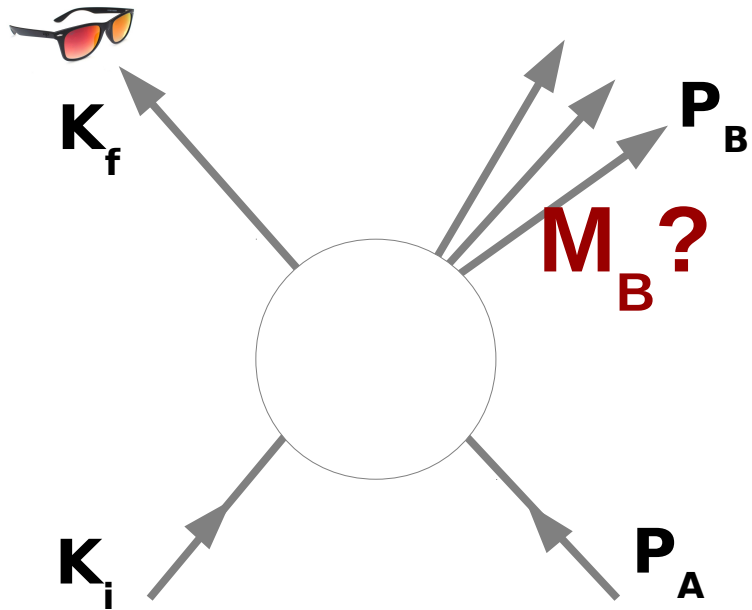
Inclusive scattering on a target at rest: only scattered lepton is detected and we know nothing about final hadronic system



4 x 4-momentum

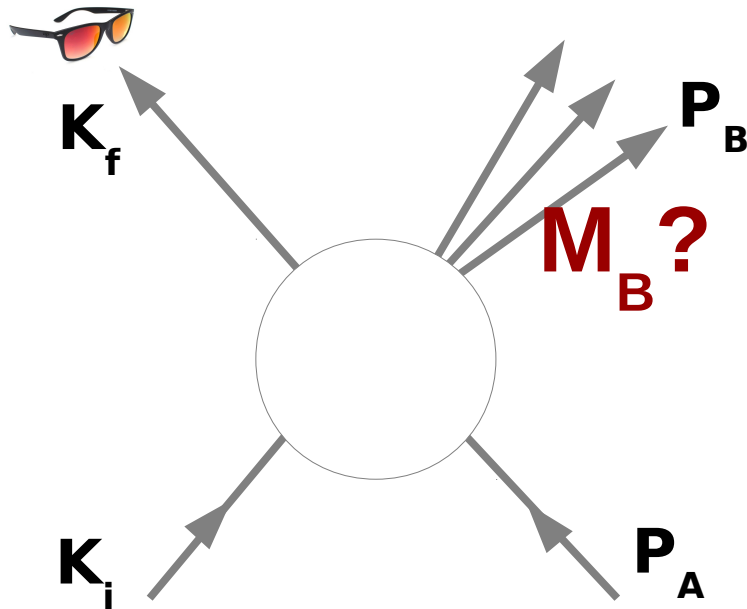
→ 16 variables

Inclusive scattering on a target at rest: only scattered lepton is detected and we know nothing about final hadronic system



4 x 4-momentum → 16 variables
1 x 4-mom. conserv. → -4 constraints
3 x ($E^2=M^2+p^2$) → -3 constraints

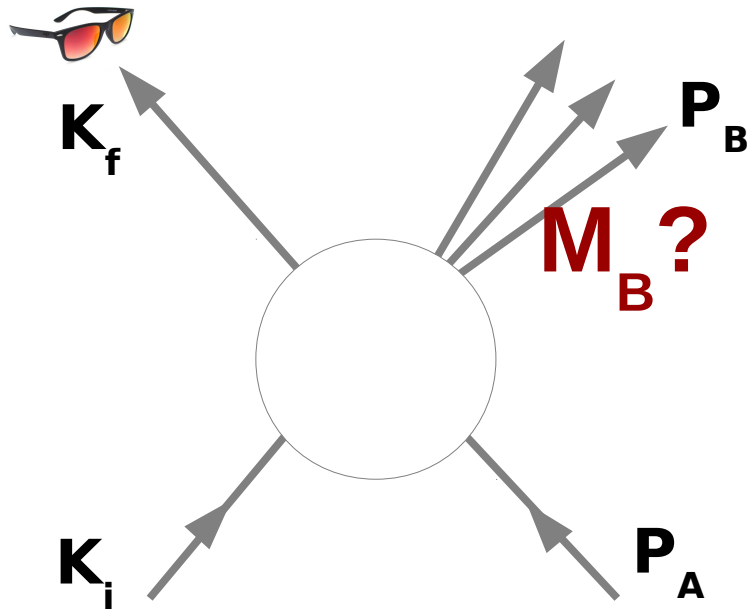
Inclusive scattering on a target at rest: only scattered lepton is detected and we know nothing about final hadronic system



- | | | |
|----------------------|---|----------------|
| 4 x 4-momentum | → | 16 variables |
| 1 x 4-mom. conserv. | → | -4 constraints |
| 3 x $(E^2=M^2+p^2)$ | → | -3 constraints |
| 3-mom. of the beam | → | -3 known |
| 3-mom. of the target | → | -3 known |
-

Independent variables left → 3

Inclusive scattering on a target at rest: only scattered lepton is detected and we know nothing about final hadronic system



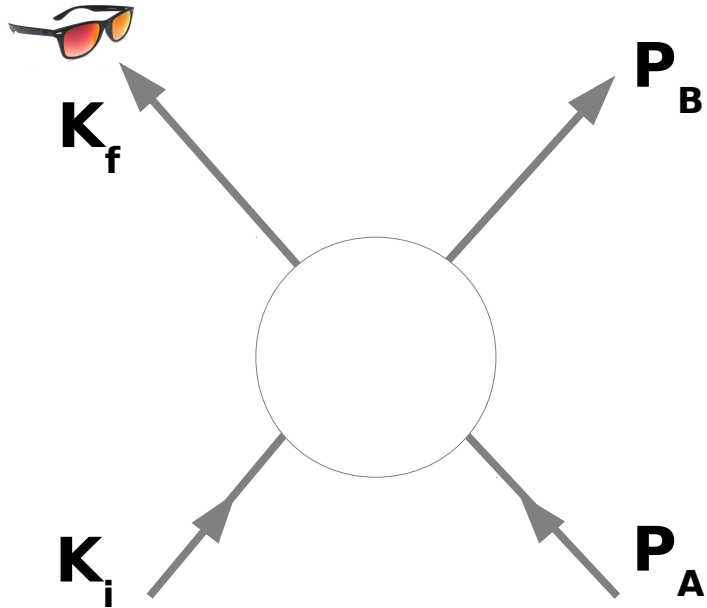
4 x 4-momentum	→	16 variables
1 x 4-mom. conserv.	→	-4 constraints
3 x ($E^2=M^2+p^2$)	→	-3 constraints
3-mom. of the beam	→	-3 known
3-mom. of the target	→	-3 known

Independent variables left → 3

We can choose the variables that we like the most as the independent variables. Typically, one chooses the lab variables of the final state:

$$\varepsilon_f, \theta_f \text{ and } \phi_f \longrightarrow \frac{d^3\sigma}{d\varepsilon_f \cos\theta_f d\phi_f}$$

The mass of the final hadronic system is known, e.g.,
elastic electron-proton scattering.

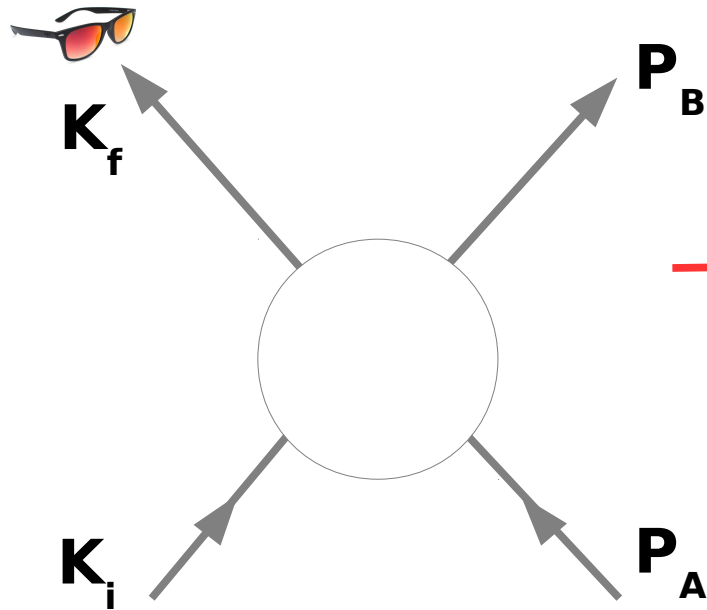


4 x 4-momentum

→ 16 variables



The mass of the final hadronic system is known, e.g.,
elastic electron-proton scattering.



4 x 4-momentum

→ 16 variables

1 x 4-mom. conserv.

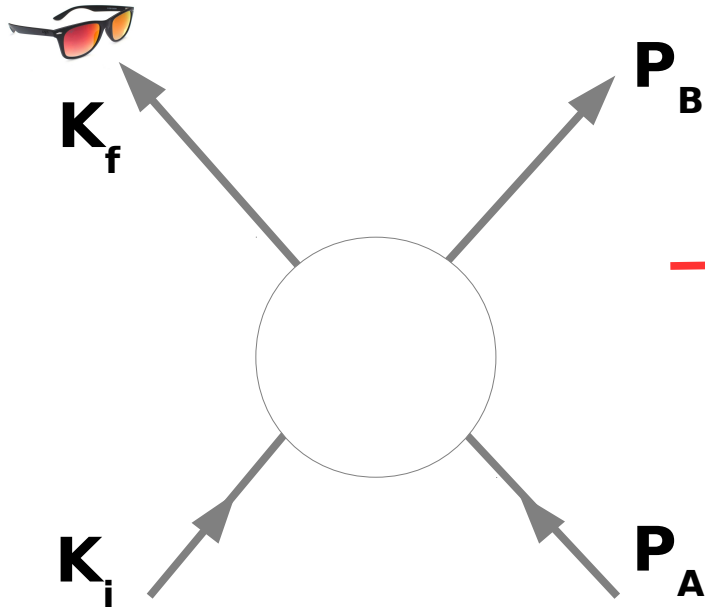
→ -4 constraints



4 x $(E^2=M^2+p^2)$

→ -4 constraints

The mass of the final hadronic system is known, e.g.,
elastic electron-proton scattering.

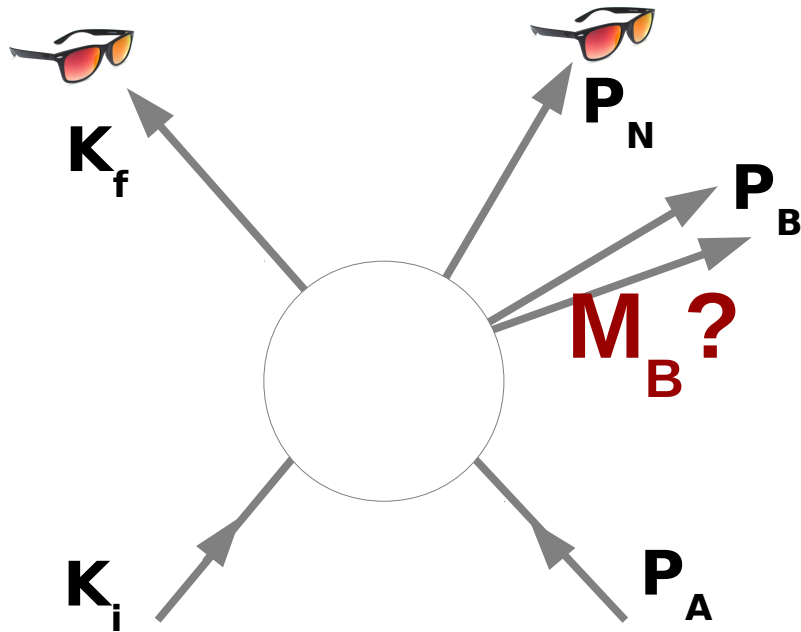


- 4 x 4-momentum → 16 variables
- 1 x 4-mom. conserv. → -4 constraints
- 4 x $(E^2=M^2+p^2)$ → -4 constraints
- 3-mom. of the beam → -3 known
- 3-mom. of the target → -3 known

Independent variables left → 2

$$\theta_f \text{ and } \phi_f \longrightarrow \frac{d^2\sigma}{d \cos \theta_f d\phi_f}$$

One hadron is detected in coincidence with the scattered lepton, e.g., **quasielastic scattering**.

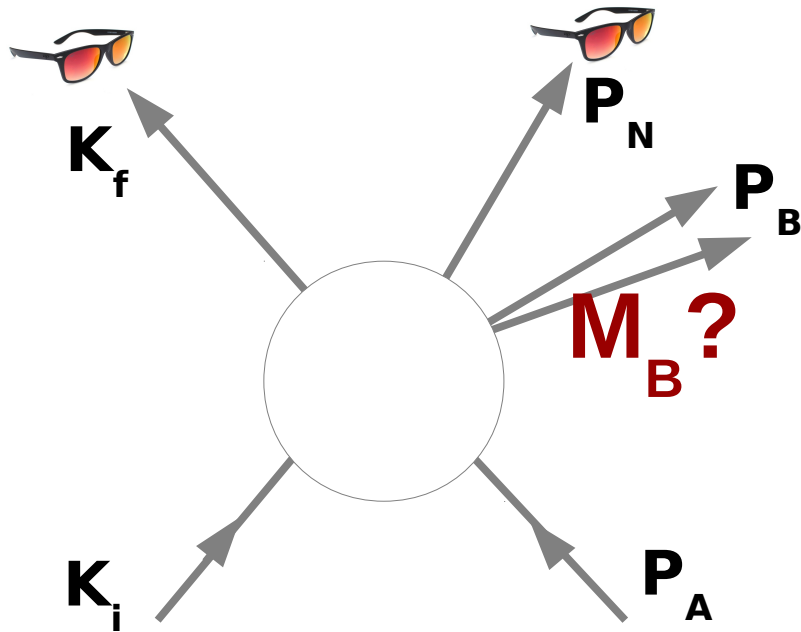


5 x 4-momentum

→ 20 variables



One hadron is detected in coincidence with the scattered lepton, e.g., **quasielastic scattering**.



5 x 4-momentum

→ 20 variables

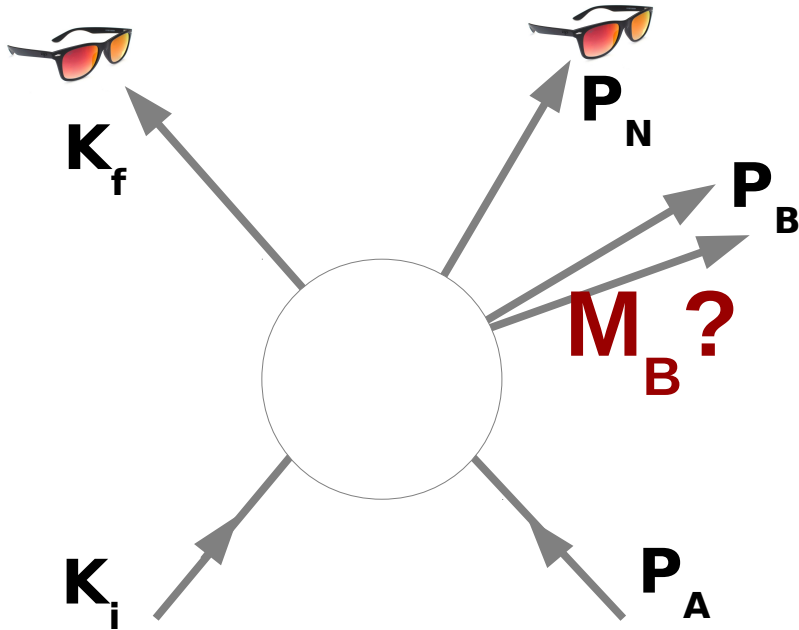
1 x 4-mom. conserv.

→ -4 constraints

4 x $(E^2=M^2+p^2)$

→ -4 constraints

One hadron is detected in coincidence with the scattered lepton, e.g., **quasielastic scattering**.

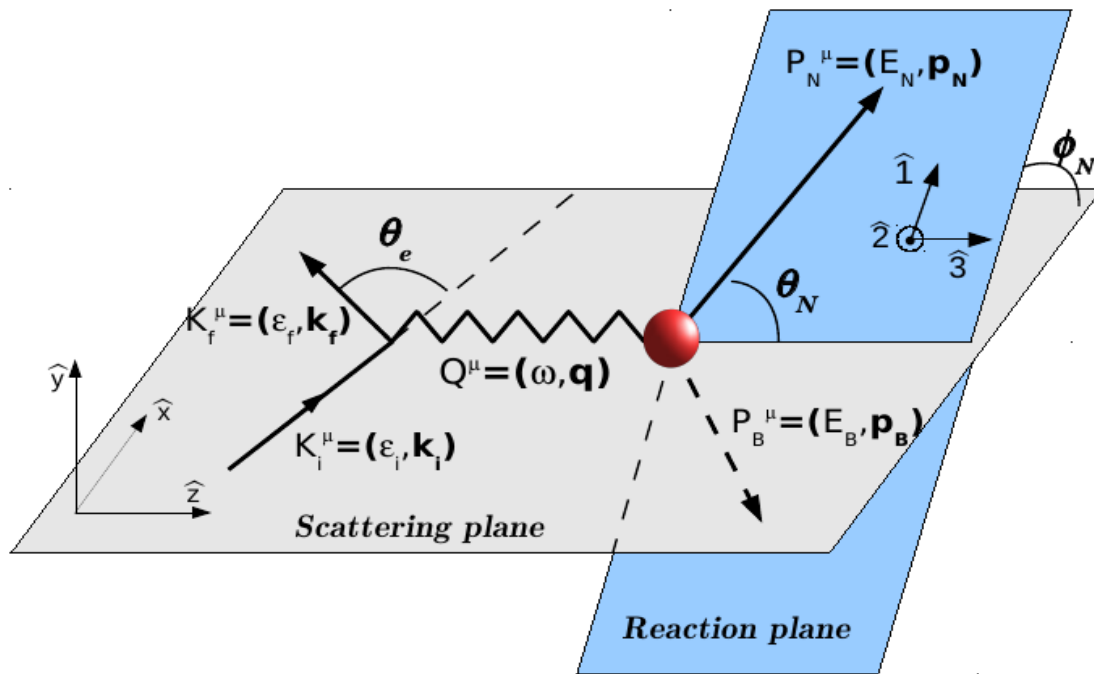


5 x 4-momentum	→	20 variables
1 x 4-mom. conserv.	→	-4 constraints
4 x $(E^2=M^2+p^2)$	→	-4 constraints
3-mom. of the beam	→	-3 known
3-mom. of the target	→	-3 known

Independent variables left → 6

$$\frac{d^6\sigma}{d\varepsilon_f d\cos\theta_f d\phi_f dp_m dE_m d\phi_N}$$

(*) E_m and p_m = Missing energy and momentum



In this reference frame ($\mathbf{q} \parallel \mathbf{z}$):

1) The cross section can be decomposed in **response functions** (Rosenbluth decomposition).

2) **Leptonic and hadronic variables are not mixed.**

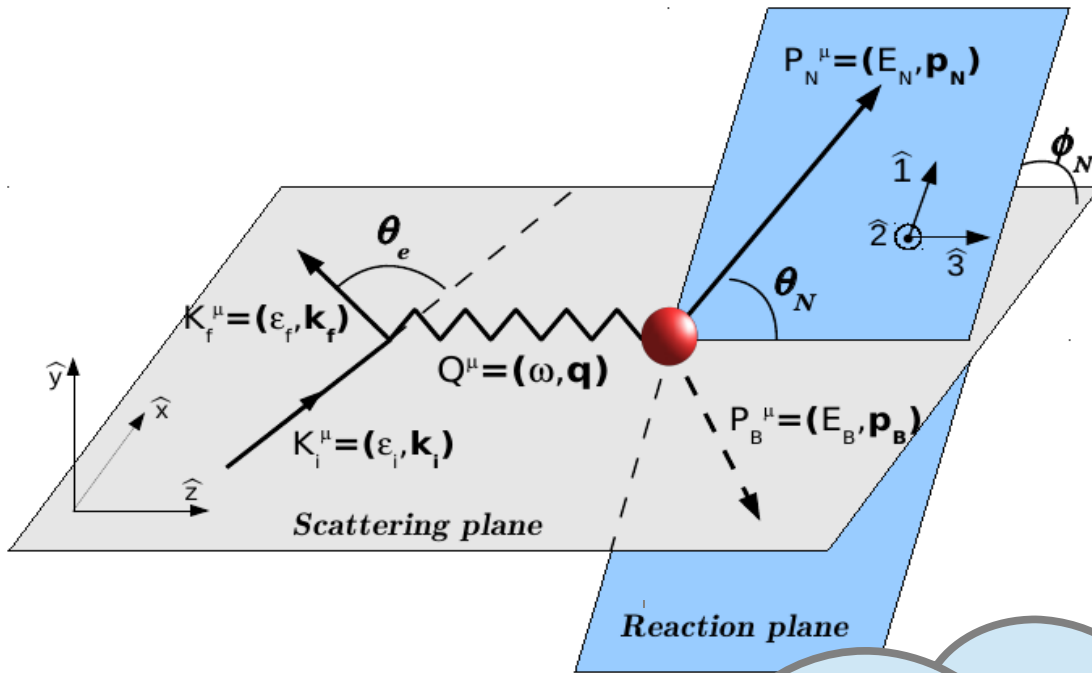
3) The ϕ_N **dependence factorizes** in terms of sines and cosines.

$$\frac{d^6\sigma}{d\phi_f d\omega dq d\Omega_N dE_m} = \sigma_{Mott} \frac{M_B M_N \rho_N}{M_A f_{rec}} \times (v_L R_L + v_T R_T + v_{TL} R_{TL} \cos \phi_N + v_{TT} R_{TT} \cos 2\phi_N)$$

v 's and R 's depend on the independent variables (I included the explicit dependence on the incoming energy)

$$v_K = v_K(\epsilon_i, \mathbf{q}, \omega)$$

$$R_K = R_K(\mathbf{q}, \omega, \theta_N, E_m)$$



In this reference frame ($\mathbf{q} \parallel \mathbf{z}$):

1) The cross section can be decomposed in **response functions** (Rosenbluth decomposition).

2) **Leptonic and hadronic variables are not mixed.**

3) The ϕ_N dependence

is in terms of sines and cosines.

$$\frac{d^6\sigma}{d\phi_f d\omega dq d\Omega_N dE_m} = \dots \times (v_L R_L + v_{TT} R_{TT} \cos 2\phi_N)$$

4 indep. variables.
If you have less...
better think about it!

v's and R's depend on the independent variables (I included the explicit dependence on the incoming energy)

$$v_K = v_K(\epsilon_i, \mathbf{q}, \omega)$$

$$R_K = R_K(\mathbf{q}, \omega, \theta_N, E_m)$$

$$\frac{d^6\sigma}{d\varepsilon_f d\Omega_f dE_m dp_m d\phi_N} \propto \ell_{\mu\nu} H^{\mu\nu}$$

$$\ell_{\mu\nu} = \overline{\sum} (j_\mu)^* j_\nu$$

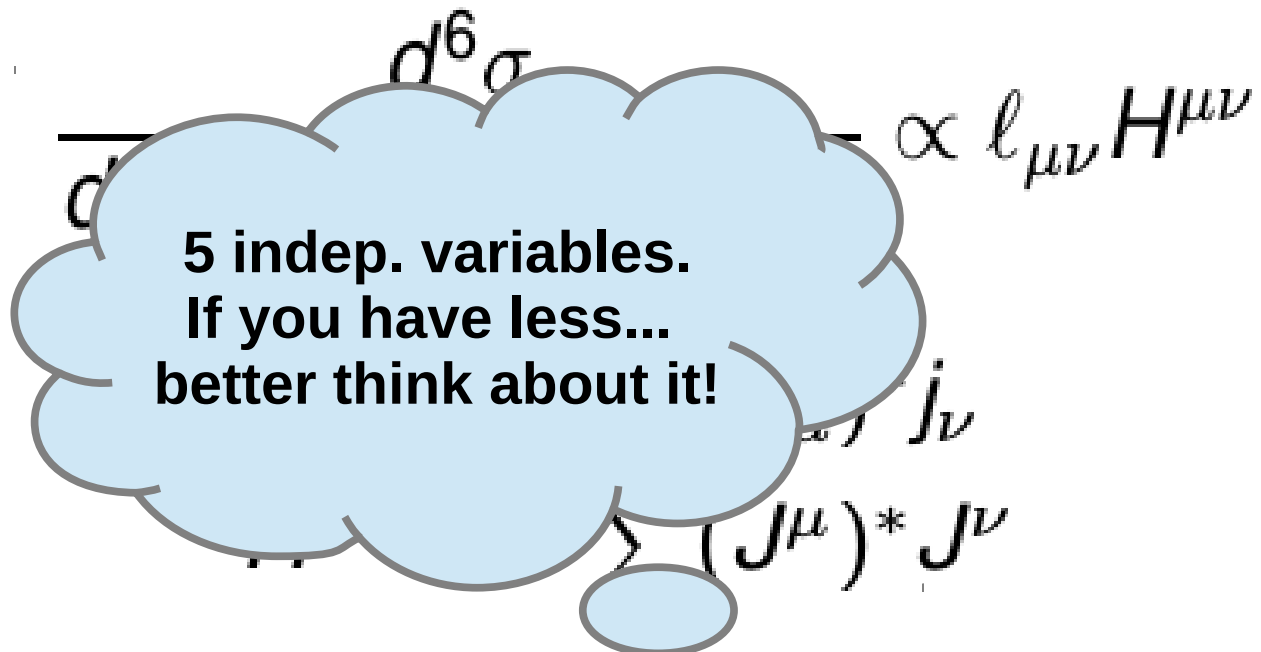
$$H^{\mu\nu} = \overline{\sum} (J^\mu)^* J^\nu$$

$$j_\mu = j_\mu(\varepsilon_i, \mathbf{q}, \omega),$$

$$J^\mu = J^\mu(\mathbf{q}, \omega, \theta_N, \phi_N, E_m)$$

If \mathbf{q} is not along \mathbf{z} , then hadronic-leptonic variables are mixed. The neutrino energy appears in the hadronic current:

$$J^\mu = J^\mu(\varepsilon_i, \mathbf{q}, \omega, \theta_N, \phi_N, E_m)$$



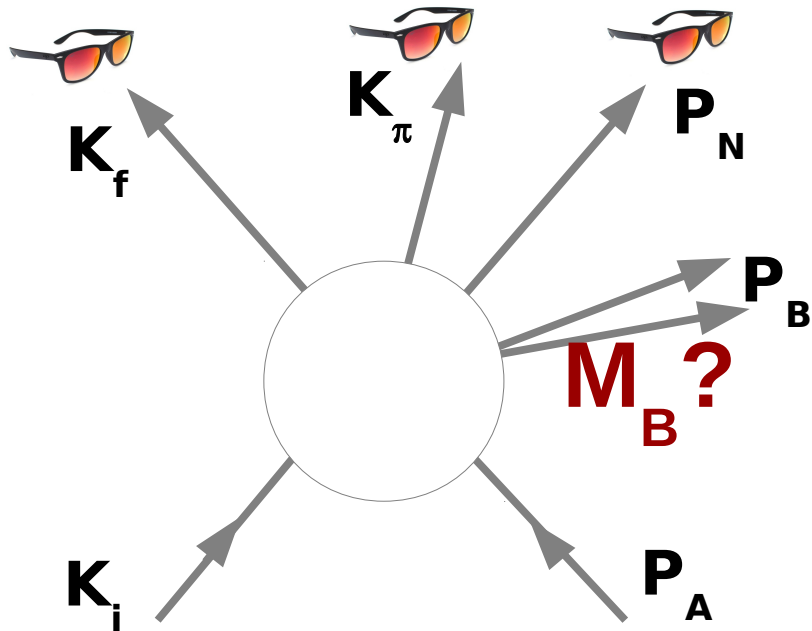
$$j_\mu = j_\mu(\varepsilon_i, \mathbf{q}, \omega),$$

$$J^\mu = J^\mu(\mathbf{q}, \omega, \theta_N, \phi_N, E_m)$$

If \mathbf{q} is not along \mathbf{z} , then hadronic-leptonic variables are mixed. The neutrino energy appears in the hadronic current:

$$J^\mu = J^\mu(\varepsilon_i, \mathbf{q}, \omega, \theta_N, \phi_N, E_m)$$

Two hadrons are detected in coincidence with the scattered lepton, e.g., **2-nucleon knockout or 1- π production.**



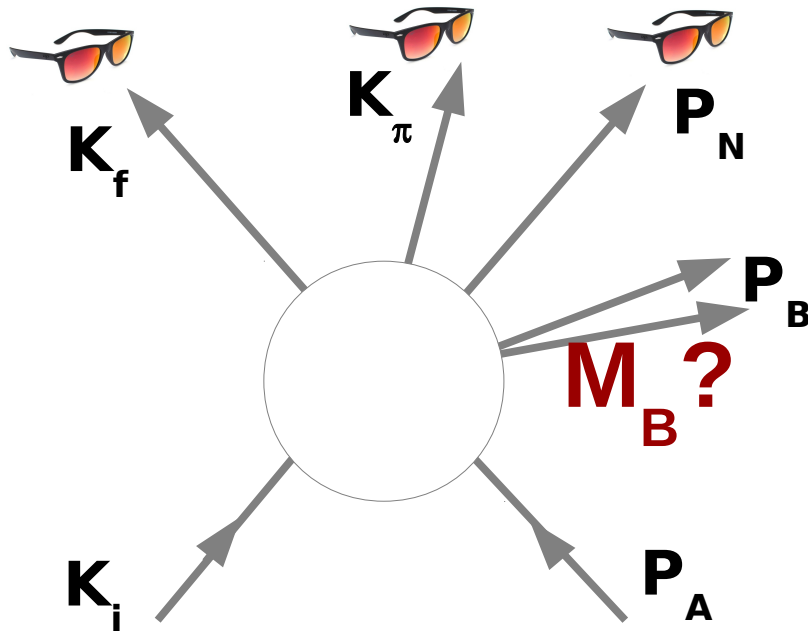
6 x 4-momentum

→ 24 variables



$$\frac{d^9 \sigma}{d\varepsilon_f d \cos \theta_f d\phi_f dE_\pi d \cos \theta_\pi d\phi_\pi d \cos \theta_N d\phi_N dE_m}$$

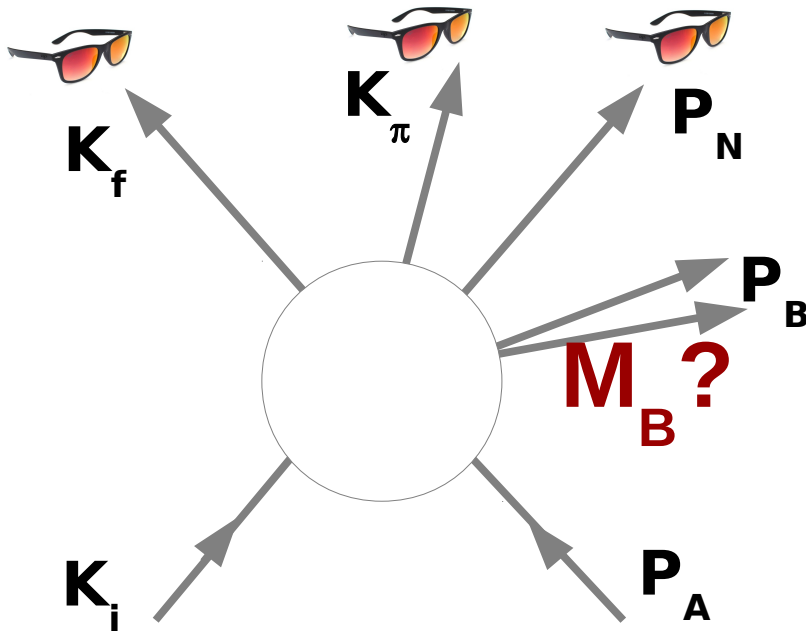
Two hadrons are detected in coincidence with the scattered lepton, e.g., **2-nucleon knockout** or **1- π production**.



6 x 4-momentum	→	24 variables
1 x 4-mom. conserv.	→	-4 constraints
5 x ($E^2=M^2+p^2$)	→	-5 constraints

$$\frac{d^9 \sigma}{d\varepsilon_f d \cos \theta_f d\phi_f dE_\pi d \cos \theta_\pi d\phi_\pi d \cos \theta_N d\phi_N dE_m}$$

Two hadrons are detected in coincidence with the scattered lepton, e.g., **2-nucleon knockout** or **1- π production**.



6 x 4-momentum	→	24 variables
1 x 4-mom. conserv.	→	-4 constraints
5 x ($E^2=M^2+p^2$)	→	-5 constraints
3-mom. of the beam	→	-3 known
3-mom. of the target	→	-3 known

Independent variables left → 9

$$\frac{d^9 \sigma}{d\varepsilon_f d \cos \theta_f d\phi_f dE_\pi d \cos \theta_\pi d\phi_\pi d \cos \theta_N d\phi_N dE_m}$$

$$\frac{d^9\sigma}{d\varepsilon_f d\Omega_f dE_\pi d\Omega_\pi d\Omega_N dE_m} \propto \ell_{\mu\nu} H^{\mu\nu}$$

$$\ell_{\mu\nu} = \overline{\sum} (j_\mu)^* j_\nu$$

$$H^{\mu\nu} = \overline{\sum} (J^\mu)^* J^\nu$$

$$j_\mu = j_\mu(\varepsilon_i, \mathbf{q}, \omega),$$

$$J^\mu = J^\mu(\mathbf{q}, \omega, E_\pi, \theta_\pi, \phi_\pi, \theta_N, \phi_N, E_m)$$

See **Donnelly**, PPNP 13, 183-236 (1985) for a smart way of factoring out the dependence on one phi-angle (using response functions).

If \mathbf{q} is not along \mathbf{z} , then:

$$J^\mu = J^\mu(\varepsilon_i, \mathbf{q}, \omega, E_\pi, \theta_\pi, \phi_\pi, \theta_N, \phi_N, E_m)$$

$$\frac{d^9 \sigma}{d\varepsilon_f d\Omega_f dE_\pi d\Omega_\pi d\Omega}$$

$$\begin{aligned} \ell_{\mu\nu} &= \overline{\Sigma} \\ H^{\mu\nu} &= \overline{\Sigma}(J^\mu) \end{aligned}$$

8 indep. variables.
If you have less...
better think about it!

$$j_\mu = j_\mu(\varepsilon_i, \mathbf{q}, \omega),$$

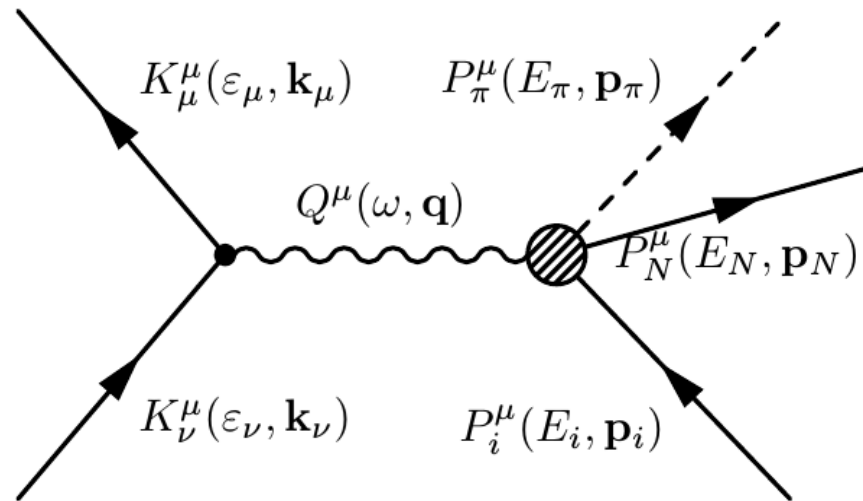
$$J^\mu = J^\mu(\mathbf{q}, \omega, E_\pi, \theta_\pi, \phi_\pi, \theta_N, \phi_N, E_m)$$

See **Donnelly**, PPNP 13, 183-236 (1985) for a smart way of factoring out the dependence on one phi-angle (using response functions).

If \mathbf{q} is not along \mathbf{z} , then:

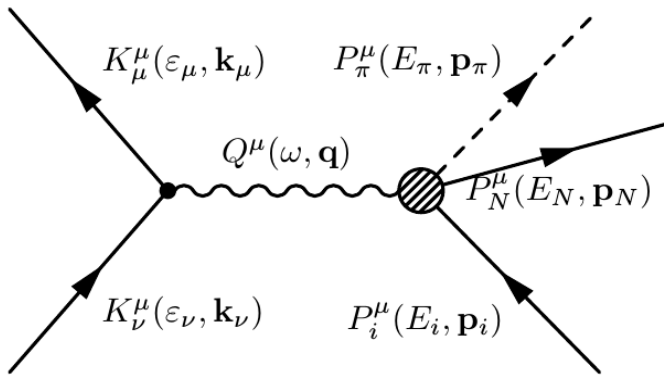
$$J^\mu = J^\mu(\varepsilon_i, \mathbf{q}, \omega, E_\pi, \theta_\pi, \phi_\pi, \theta_N, \phi_N, E_m)$$

Single-Pion Production off the nucleon



RGJ et al., PRD 95, 113007 (2017)

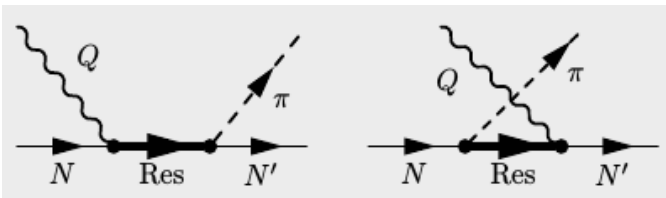
Low-energy model



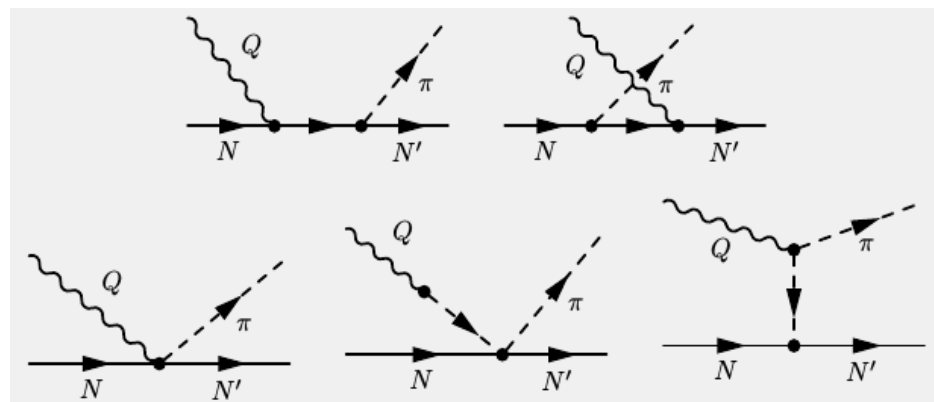
Low-energy model for pion-production on the nucleon:
ChPT background + resonances
Valencia model
 (PRD 76 (2007) 033005; PRD 87 (2013) 113009)

Resonances:

P33(1232), D13(1520),
 S11(1535), P11(1440)

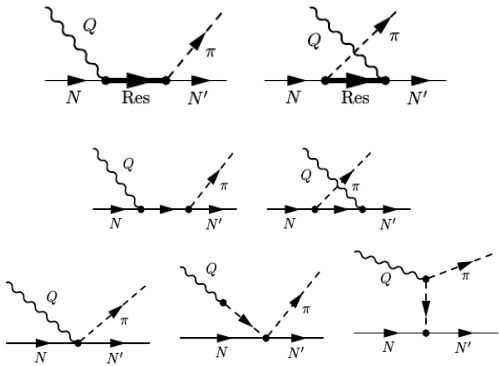


ChPT background:



The Problem

Low-energy model
(resonances + ChPT bg)



Unphysical predictions at large invariant masses.

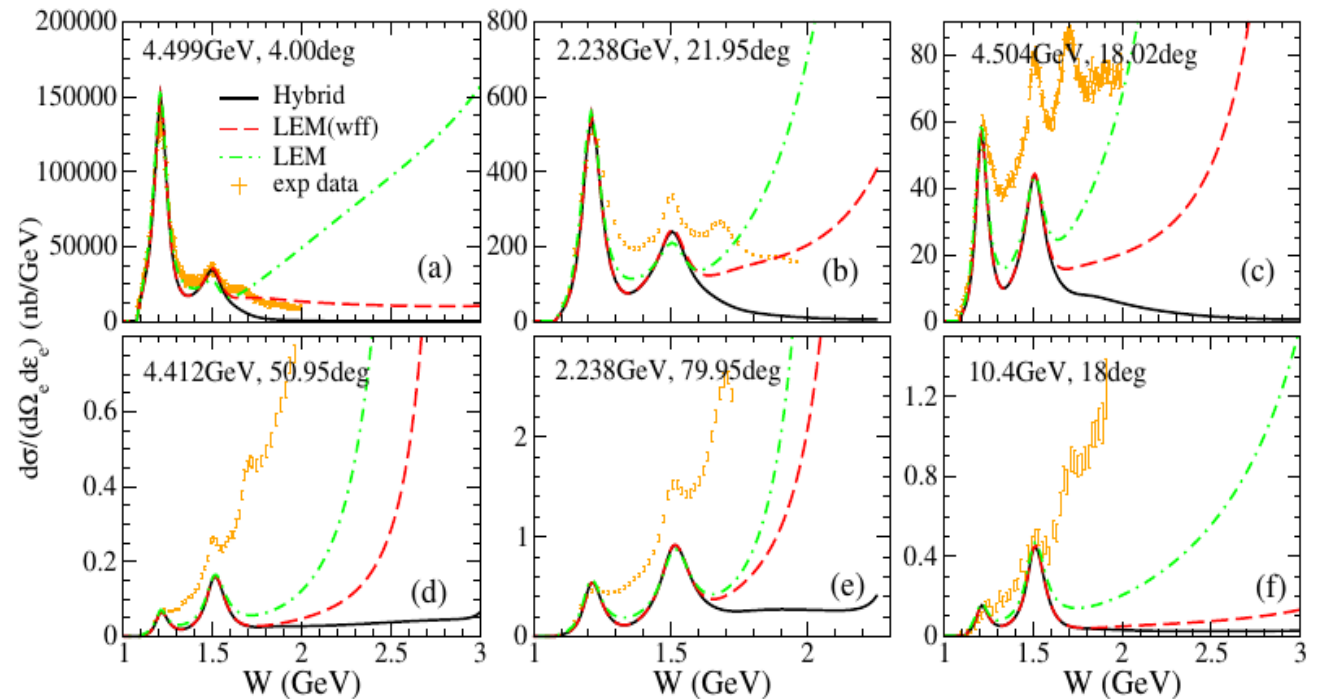
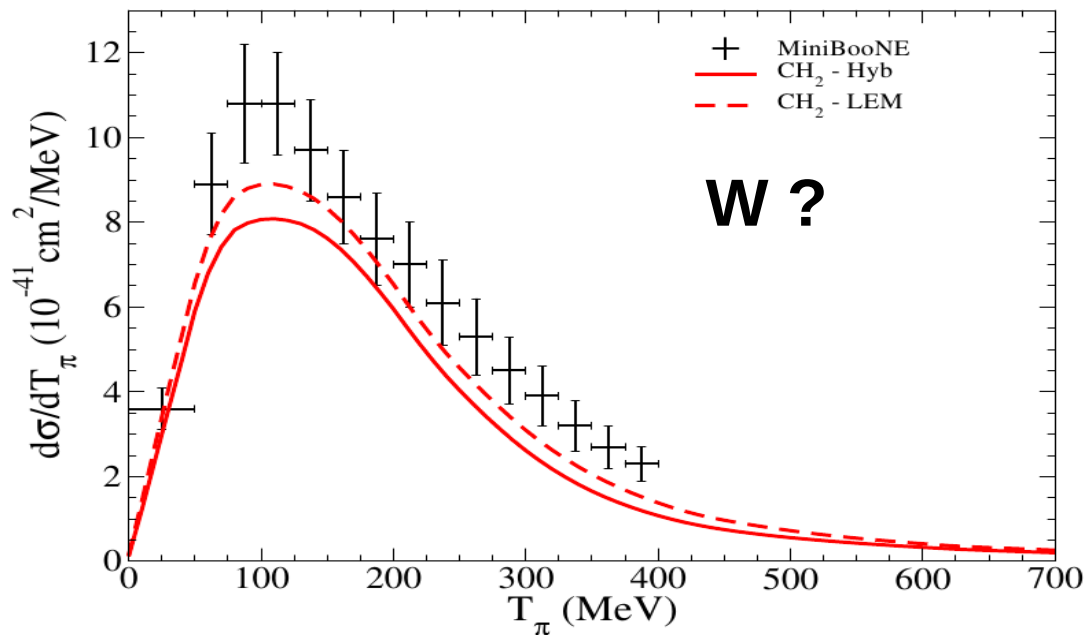


Figure: The model overshoots inclusive electron-proton scattering data.

The Problem



W values? We don't know...
+ Fermi motion
+ Flux-folding

Therefore, we need reliable predictions in:

+ the **resonance region**
 $W < 2 \text{ GeV}$,
+ the **high-energy** energy
region $W > 2 \text{ GeV}$

Regge Theory

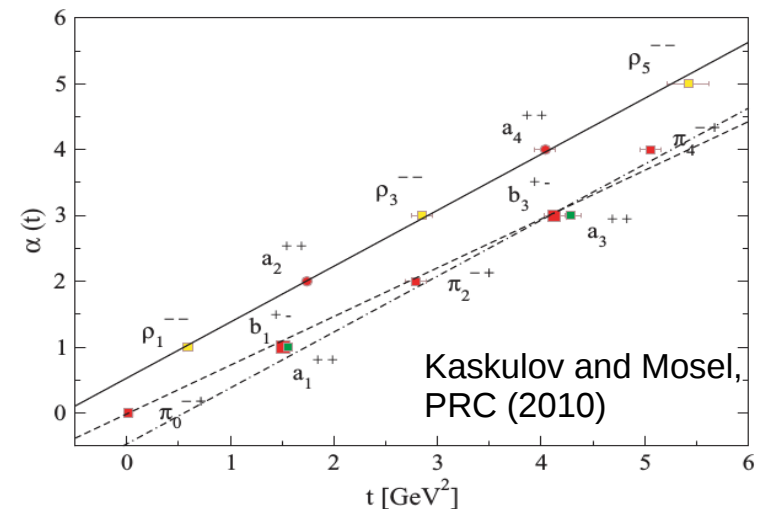
Based on unitarity, causality and crossing symmetry, Regge Theory provides the **high energy ($s \rightarrow \infty$) behavior** of the amplitude:

$$A(s,t) \sim \beta(t) s^{\alpha(t)}$$

Regge theory does not predict the **t-dependence** of the amplitude.

For that, one needs a model.

$\alpha(t)$: Families or Regge trajectories

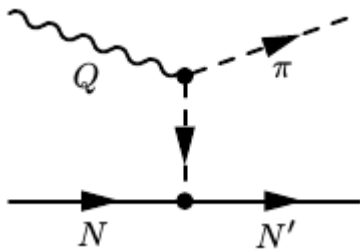


High-energy model

Regge approach for the vector amplitudes.

We use the approach of **Guidal, Laget, and Vanderhaeghen** [NPA627, 645 (1997)], originally developed for pion photoproduction ($Q^2 = 0$):

- 1) Feynman **meson-exchange diagrams** are reggeized.



$$\frac{1}{t - m_{\pi}^2}$$

The pion propagator is replaced by the Regge trajectory of the pion family

$$\mathcal{P}_{\pi}(t, s) = -\alpha'_{\pi} \varphi_{\pi}(t) \Gamma[-\alpha_{\pi}(t)] (\alpha'_{\pi} s)^{\alpha_{\pi}(t)}$$

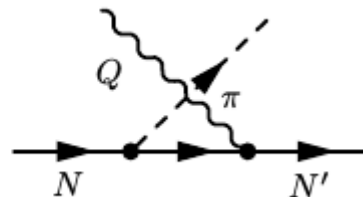
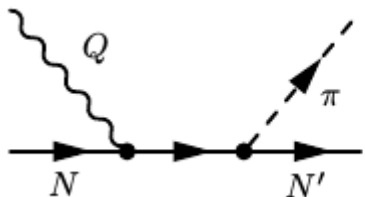
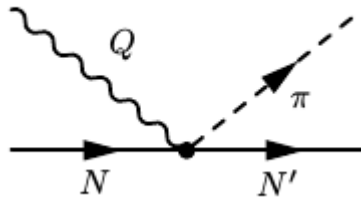
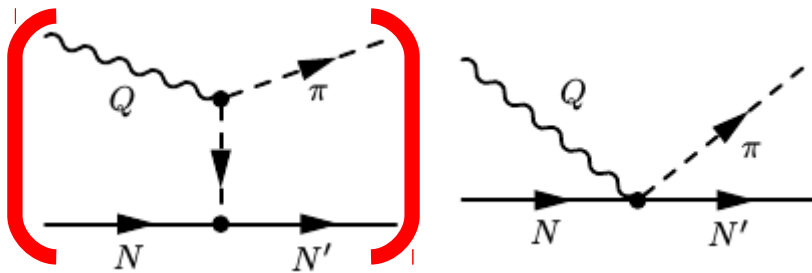
High-energy model

Regge approach for the vector amplitudes.

We use the approach of **Guidal, Laget, and Vanderhaeghen** [NPA627, 645 (1997)], originally developed for pion photoproduction ($Q^2 = 0$):

1) Feynman **meson-exchange diagrams** are reggeized.

2) s-channel and u-channel diagrams are included to keep **Conservation of Vector Current**.



$$\frac{1}{t - m_\pi^2}$$

The pion propagator is replaced by the Regge trajectory of the pion family

$$\mathcal{P}_\pi(t, s) = -\alpha'_\pi \varphi_\pi(t) \Gamma[-\alpha_\pi(t)] (\alpha'_\pi s)^{\alpha_\pi(t)}$$

High-energy model: $N(e, e'\pi)N'$ results

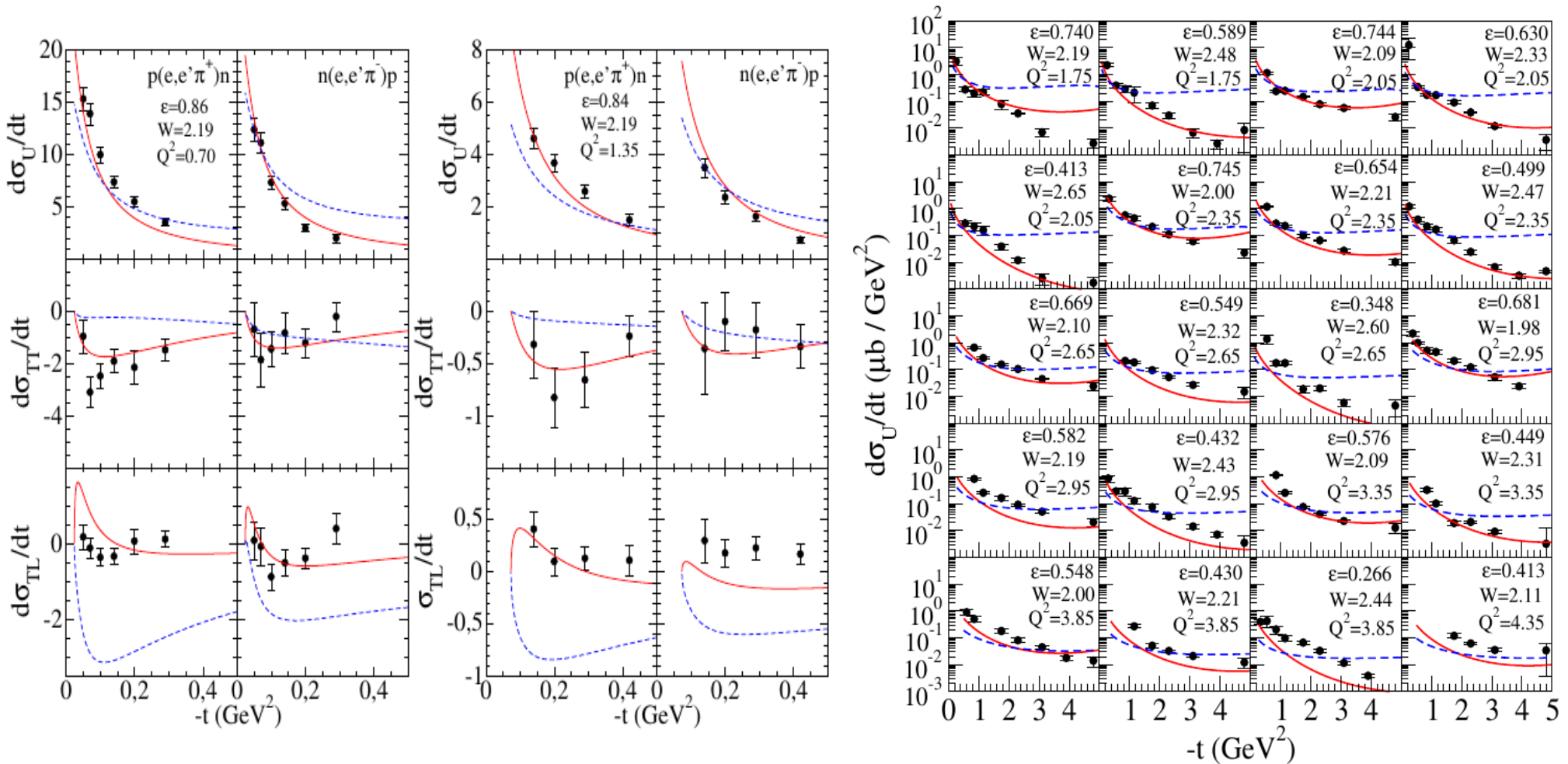


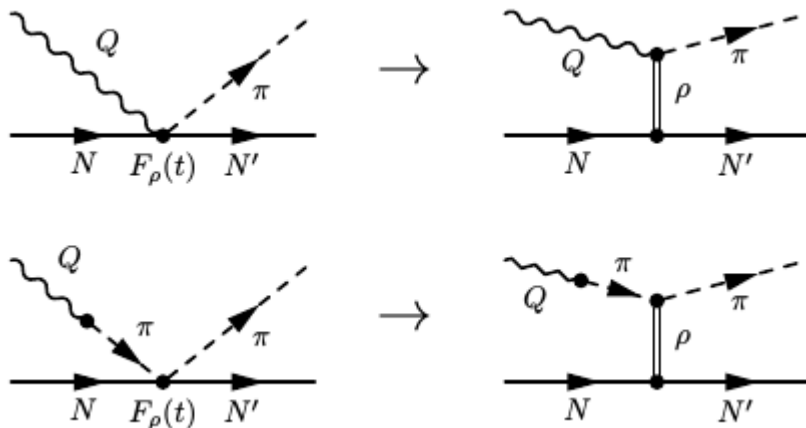
Figure: High-energy model (red lines), low-energy model (blue lines) and electron-induced single-pion production data.

High-energy model

Regge approach for the axial amplitudes.

We need meson exchange diagrams to apply the reggeization procedure of the current.

Effective rho-exchange diagrams. This allows us to consider the rho-exchange as the main Regge trajectory in the axial current.



$$O_{CT\rho}^\mu = i\mathcal{I} \frac{m_\rho^2}{m_\rho^2 - t} F_{A\rho\pi}(Q^2) \frac{1}{\sqrt{2}f_\pi} \times \left(\gamma^\mu + i \frac{\kappa_\rho}{2M} \sigma^{\mu\nu} K_{t,\nu} \right).$$

We consider $\kappa_\rho = 0$ so that the low-energy model amplitude is recovered.

The propagator of the rho is replaced by the Regge trajectory of the **rho family**:

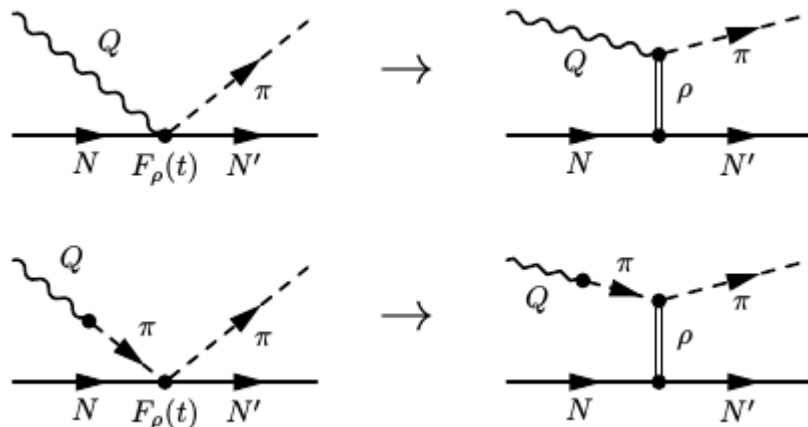
$$\mathcal{P}_\rho(t, s) = -\alpha'_\rho \varphi_\rho(t) \Gamma[1 - \alpha_\rho(t)] (\alpha'_\rho s)^{\alpha_\rho(t) - 1}$$

High-energy model

Regge approach for the axial amplitudes.

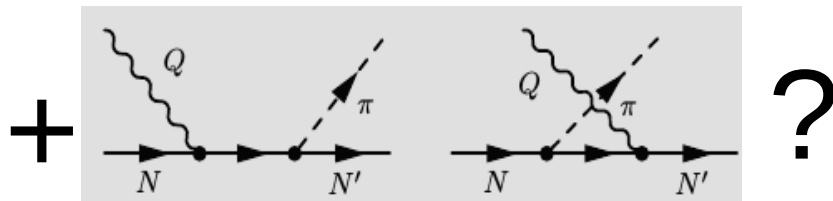
We need meson exchange diagrams to apply the reggeization procedure of the current.

Effective rho-exchange diagrams. This allows us to consider the rho-exchange as the main Regge trajectory in the axial current.



$$O_{CT\rho}^\mu = i\mathcal{I} \frac{m_\rho^2}{m_\rho^2 - t} F_{A\rho\pi}(Q^2) \frac{1}{\sqrt{2}f_\pi} \times \left(\gamma^\mu + i \frac{\kappa_\rho}{2M} \sigma^{\mu\nu} K_{t,\nu} \right).$$

We consider $\kappa_\rho = 0$ so that the low-energy model amplitude is recovered.



High-energy model: results

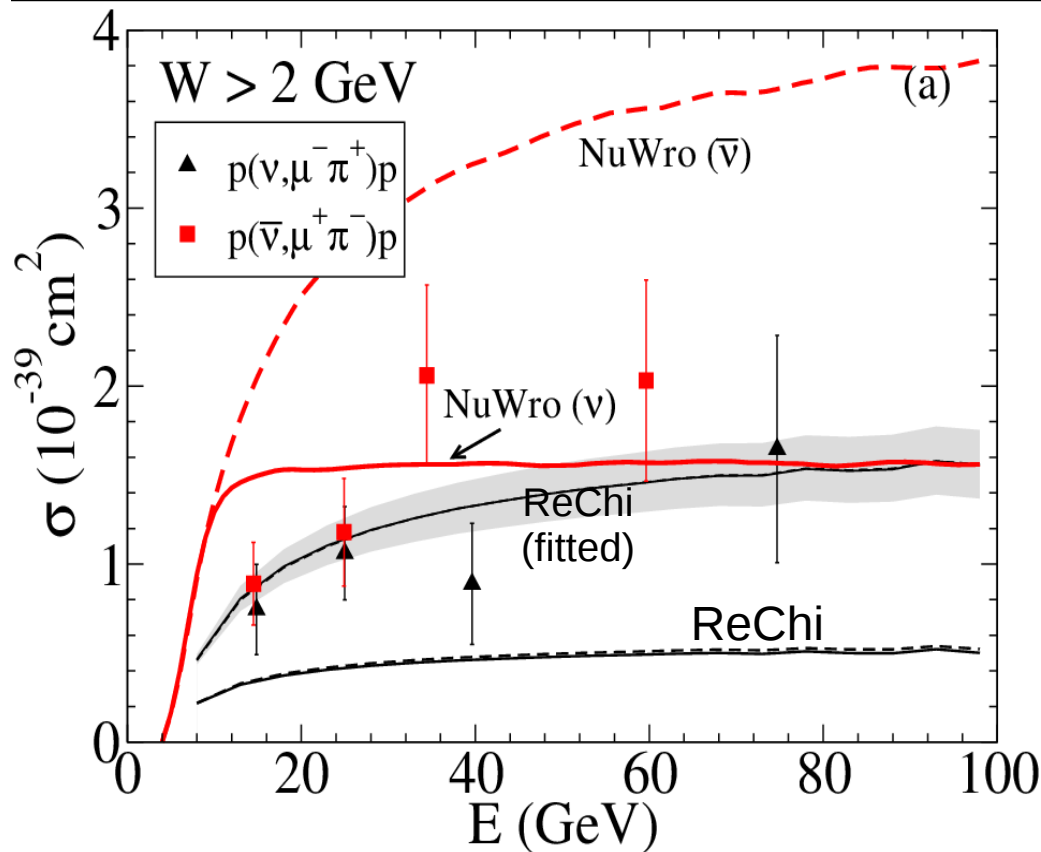
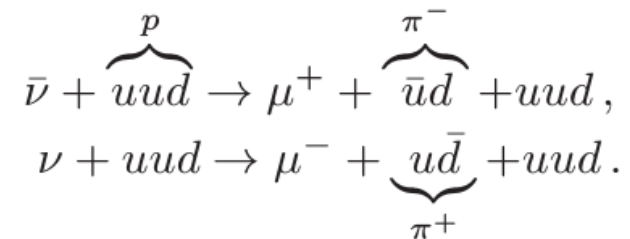


Figure: ReChi model and NuWro predictions are compared with high energy cross section data for neutrino and antineutrino reactions (Note the high energy cut $W > 2$ GeV !!). Data from Allen et al. NPB264, 221 (1986).

NuWro: Based on DIS formalism and PYTHIA for hadronization.

Antineutrino cross section is ~ 2 the neutrino one:



High-energy model: results

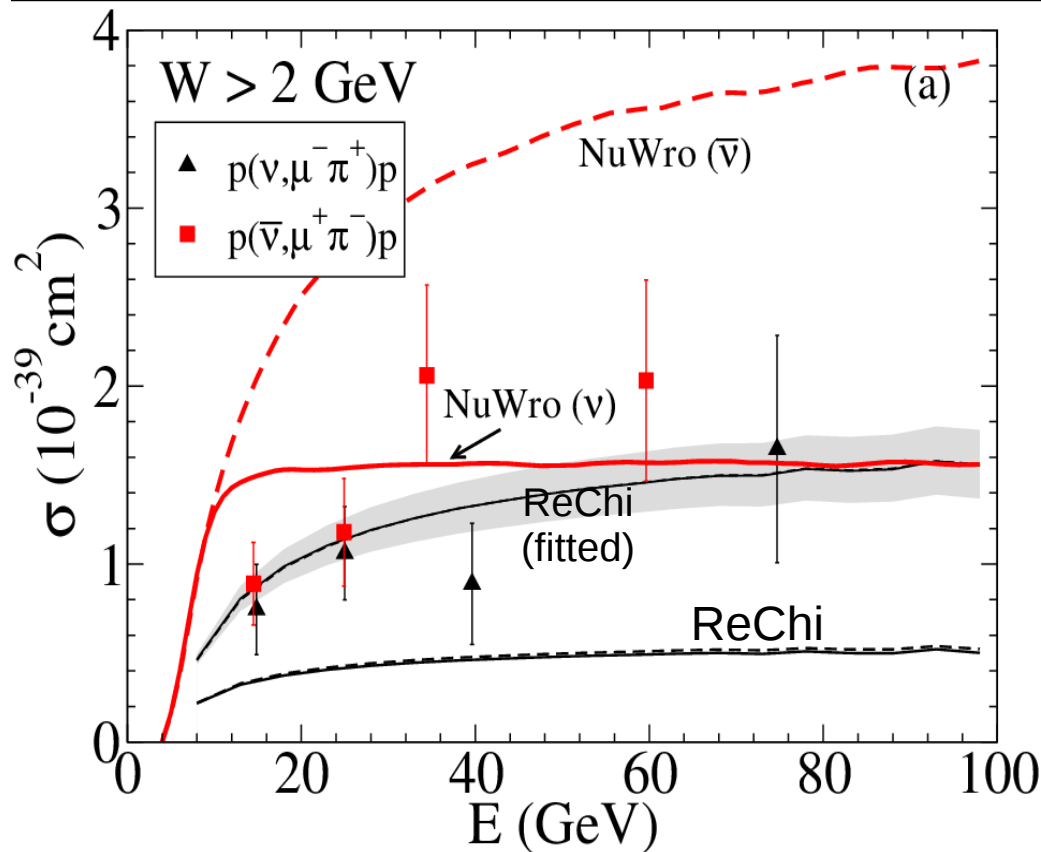
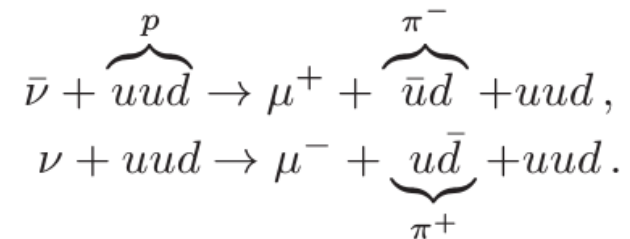


Figure: ReChi model and NuWro predictions are compared with high energy cross section data for neutrino and antineutrino reactions (Note the high energy cut $W > 2$ GeV !!). Data from Allen et al. NPB264, 221 (1986).

NuWro: Based on DIS formalism and PYTHIA for hadronization.

Antineutrino cross section is ~ 2 the neutrino one:



ReChi model: One free parameter in the boson-nucleon-nucleon vertex

$$G_A[Q^2, s(u)] = g_A \left(1 + \frac{Q^2}{\Lambda_{Apn^*} [s(u)]^2} \right)^{-2}$$

$$\Lambda_{Apn^*}(s) = \Lambda_{Apn} + (\Lambda_{\infty}^A - \Lambda_{Apn}) \left(1 - \frac{M^2}{s} \right)$$

$$\Lambda_{\infty}^A = (7.20 \pm_{1.32}^{2.09}) \text{ GeV} !!!$$

Hybrid model: results

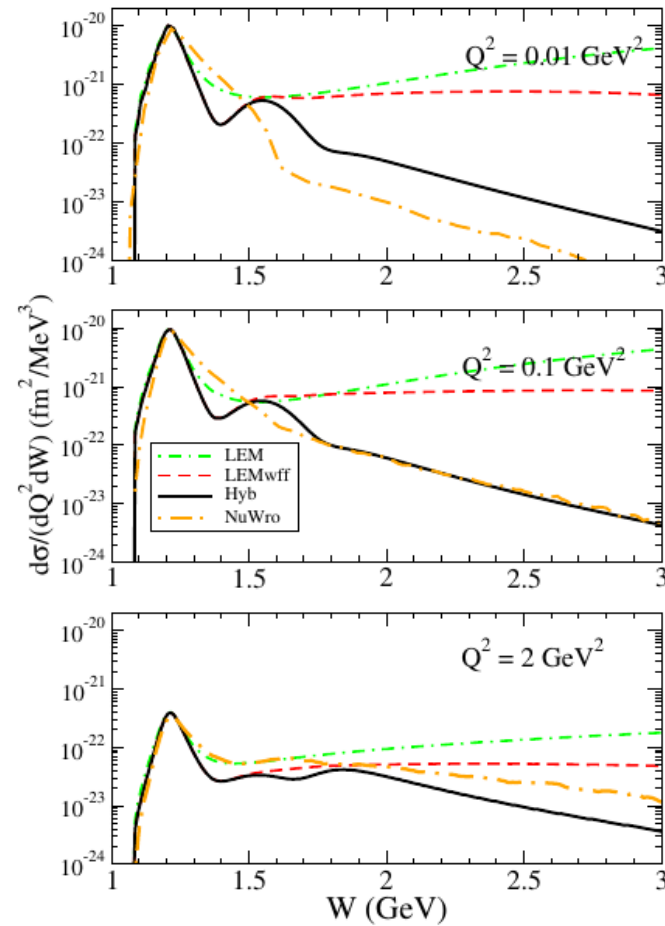
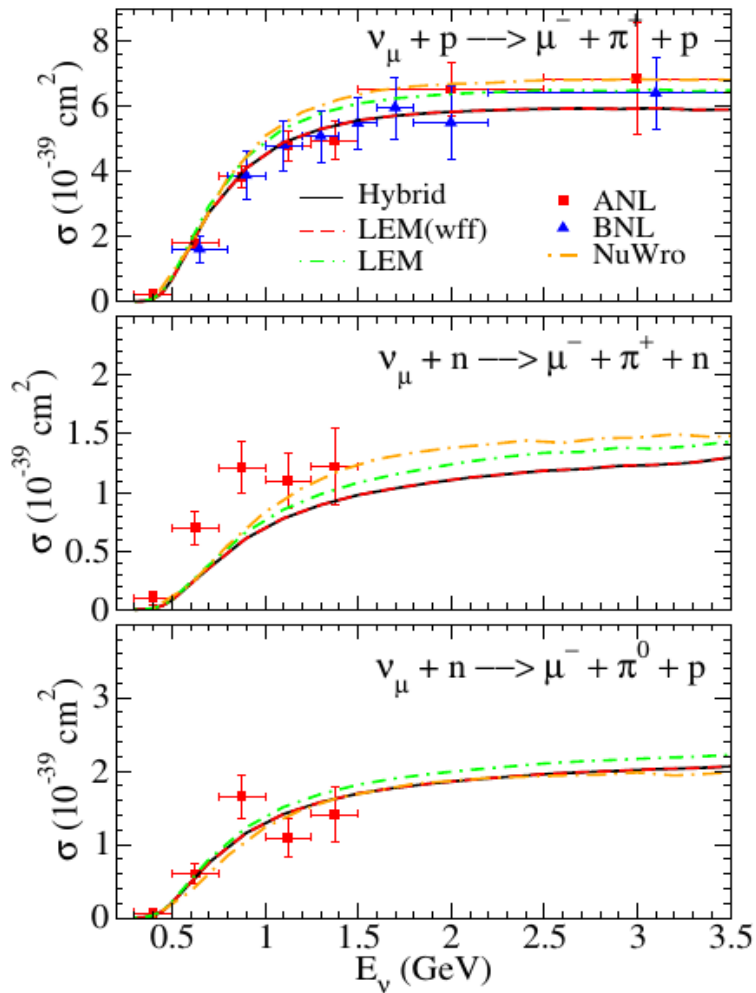


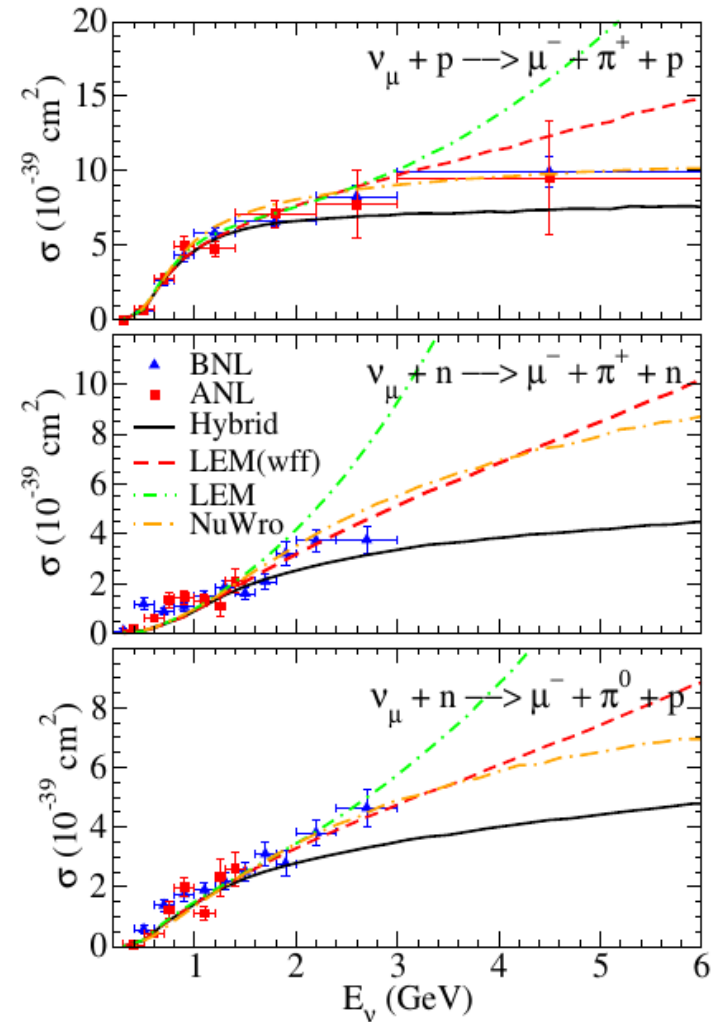
FIG. 21. (Color online) Different model predictions for the differential cross section $d\sigma/(dQ^2 dW)$, for the channel $p(\nu_\mu, \mu^- \pi^+)p$. The incoming neutrino energy is fixed to $E_\nu = 10$ GeV .

Hybrid model: results

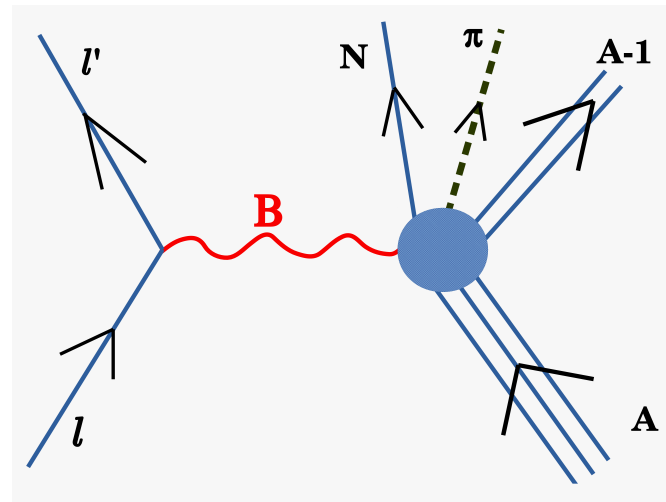
W < 1.4 GeV



No cut in W



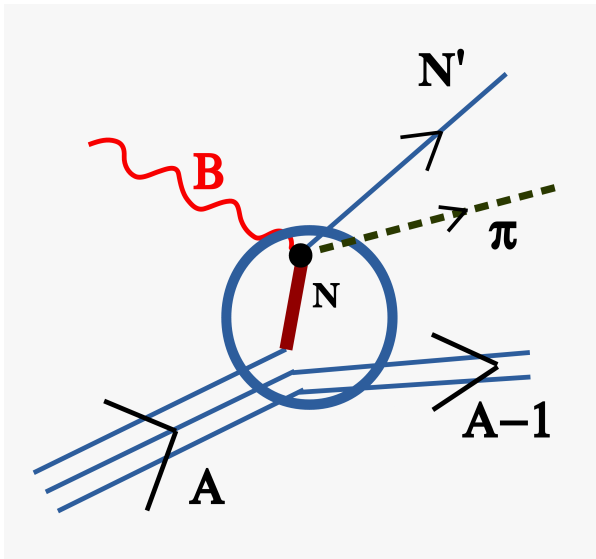
Electroweak one-pion production on nuclei



RGJ et al., arXiv:1710.08374 [nucl-th]

Relativistic mean field model

Relativistic Impulse Approximation



$$J_{had}^{\mu} = \sum_i^A \int d\mathbf{r} \bar{\Psi}_F(\mathbf{r}) \phi^*(\mathbf{r}) \hat{O}_{one-body}^{\mu}(\mathbf{r}) \Psi_B(\mathbf{r}) e^{i\mathbf{q}\cdot\mathbf{r}}$$

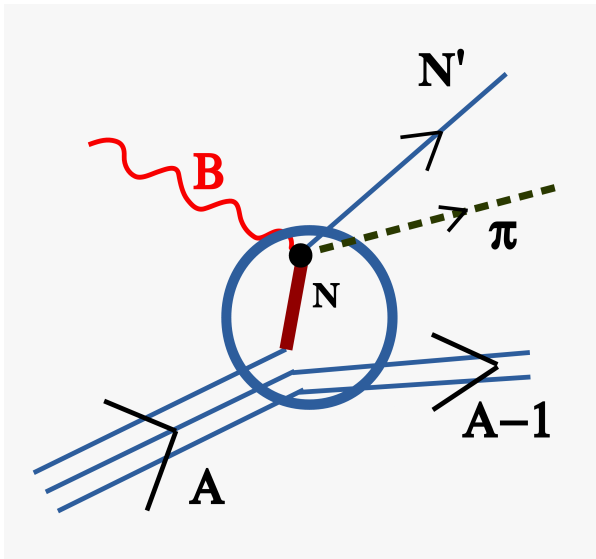
Relativistic mean-field wave functions

$$\frac{d^8\sigma}{d\varepsilon_f d\Omega_f dE_{\pi} d\Omega_{\pi} d\Omega_N} = \frac{m_i m_f}{(2\pi)^8} \frac{M_N p_N k_{\pi}}{E_N f_{rec}} \frac{k_f}{\varepsilon_i} \sum_{fi} |\mathcal{M}_{fi}|^2$$

8-fold differential cross section:
Computationally very demanding

Relativistic mean field model

Relativistic Impulse Approximation



Plane waves (for the moment...)

$$J_{had}^{\mu} = \sum_i^A \int d\mathbf{r} \bar{\Psi}_F(\mathbf{r}) \phi^*(\mathbf{r}) \hat{O}_{one-body}^{\mu}(\mathbf{r}) \Psi_B(\mathbf{r}) e^{i\mathbf{q}\cdot\mathbf{r}}$$

Relativistic mean-field wave functions

$$\frac{d^8\sigma}{d\varepsilon_f d\Omega_f dE_{\pi} d\Omega_{\pi} d\Omega_N} = \frac{m_i m_f}{(2\pi)^8} \frac{M_N p_N k_{\pi}}{E_N f_{rec}} \frac{k_f}{\varepsilon_i} \sum_{fi} |\mathcal{M}_{fi}|^2$$

8-fold differential cross section:
Computationally very demanding

Relativistic mean-field model

RMF model provides a microscopic description of the ground state of finite nuclei which is consistent with Quantum Mechanics, Special Relativity and symmetries of strong interaction.

The starting point is a Lorentz covariant Lagrangian density

$$\begin{aligned} \mathcal{L} = & \bar{\Psi} (i\gamma_{\mu}\partial^{\mu} - M) \Psi + \frac{1}{2} (\partial_{\mu}\sigma\partial^{\mu}\sigma - m_{\sigma}^2\sigma^2) - U(\sigma) \\ & - \frac{1}{4}\Omega_{\mu\nu}\Omega^{\mu\nu} + \frac{1}{2}m_{\omega}^2\omega_{\mu}\omega^{\mu} - \frac{1}{4}\mathbf{R}_{\mu\nu}\mathbf{R}^{\mu\nu} + \frac{1}{2}m_{\rho}^2\rho_{\mu}\rho^{\mu} - \frac{1}{4}F_{\mu\nu}F^{\mu\nu} \\ & - g_{\sigma}\bar{\Psi}\sigma\Psi - g_{\omega}\bar{\Psi}\gamma_{\mu}\omega^{\mu}\Psi - g_{\rho}\bar{\Psi}\gamma_{\mu}\boldsymbol{\tau}\boldsymbol{\rho}^{\mu}\Psi - g_e\frac{1+\tau_3}{2}\bar{\Psi}\gamma_{\mu}A^{\mu}\Psi. \end{aligned}$$

Extension of the original σ - ω Walecka model (Ann. Phys.83,491 (1974)).

where

$$\Omega^{\mu\nu} = \partial^{\mu}\omega^{\nu} - \partial^{\nu}\omega^{\mu},$$

$$\mathbf{R}^{\mu\nu} = \partial^{\mu}\boldsymbol{\rho}^{\nu} - \partial^{\nu}\boldsymbol{\rho}^{\mu},$$

$$F^{\mu\nu} = \partial^{\mu}A^{\nu} - \partial^{\nu}A^{\mu}.$$

$$U(\sigma) = \frac{1}{3}g_2\sigma^3 + \frac{1}{4}g_3\sigma^4$$

Main approximations:

1) Mean-field approximation:

$$\omega_{\mu} \rightarrow \langle \omega_{\mu} \rangle \quad \sigma \rightarrow \langle \sigma \rangle \quad \rho_{\mu} \rightarrow \langle \rho_{\mu} \rangle$$

2) Static limit:

$$\partial^0\omega_0 = \partial^0\rho_0 = \partial^0\sigma = 0 \quad \omega_{\mu} = \delta_{\mu 0}\omega_0, \quad \rho_{\mu} = \delta_{\mu 0}\rho_0$$

3) Spherical symmetry for finite nuclei:

$$\omega_0 = \omega_0(r) \quad \rho_0 = \rho_0(r) \quad \sigma = \sigma(r)$$

Relativistic mean-field model

Dirac equation for nucleons (eq. of motion for the barionic fields):

$$[-i\boldsymbol{\alpha} \cdot \nabla + V(r) + \beta(M + S(r))]\Psi_i(\mathbf{r}) = E_i\Psi_i(\mathbf{r})$$

where the scalar (S) and vector (V) potential are given by:

$$S(r) = g_\sigma\sigma(r),$$

$$V(r) = g_\omega\omega^0(r) + g_\rho\tau_3\rho_3^0(r) + e\frac{1 + \tau_3}{2}A^0(r)$$

Eqs. of motion for the mesons and the photon:

$$[-\nabla^2 + m_\sigma^2]\sigma(r) = -g_\sigma\rho_s(r) - g_2\sigma^2(r) - g_3\sigma^3(r),$$

$$[-\nabla^2 + m_\omega^2]\omega^0(r) = -g_\omega\rho_B(r),$$

$$[-\nabla^2 + m_\rho^2]\rho_3^0(r) = -g_\rho\rho_\rho(r),$$

$$-\nabla^2 A^0 = e\rho_c,$$

Current densities

$$\rho_s(r) = \sum_i^A \bar{\Psi}_i(\mathbf{r})\Psi_i(\mathbf{r}),$$

$$\rho_B(r) = \sum_i^A \Psi_i^\dagger(\mathbf{r})\Psi_i(\mathbf{r}),$$

$$\rho_\rho(r) = \sum_i^A \Psi_i^\dagger(\mathbf{r})\tau_3\Psi_i(\mathbf{r})$$

$$\rho_c(r) = \sum_i^A \Psi_i^\dagger(\mathbf{r})\frac{1 + \tau_3}{2}\Psi_i(\mathbf{r})$$

Solution of the couple equations for the fields in a self-consistent way.

Relativistic mean-field model

In general, the parameters are fit to reproduce some general properties of some closed shell spherical nuclei and nuclear matter.

Parameters for the NLSH model (fitted to the mean charge radius, binding energy and neutron radius of the ^{16}O , ^{40}Ca , ^{90}Zr , ^{116}Sr , ^{124}Sn and ^{208}Pb).

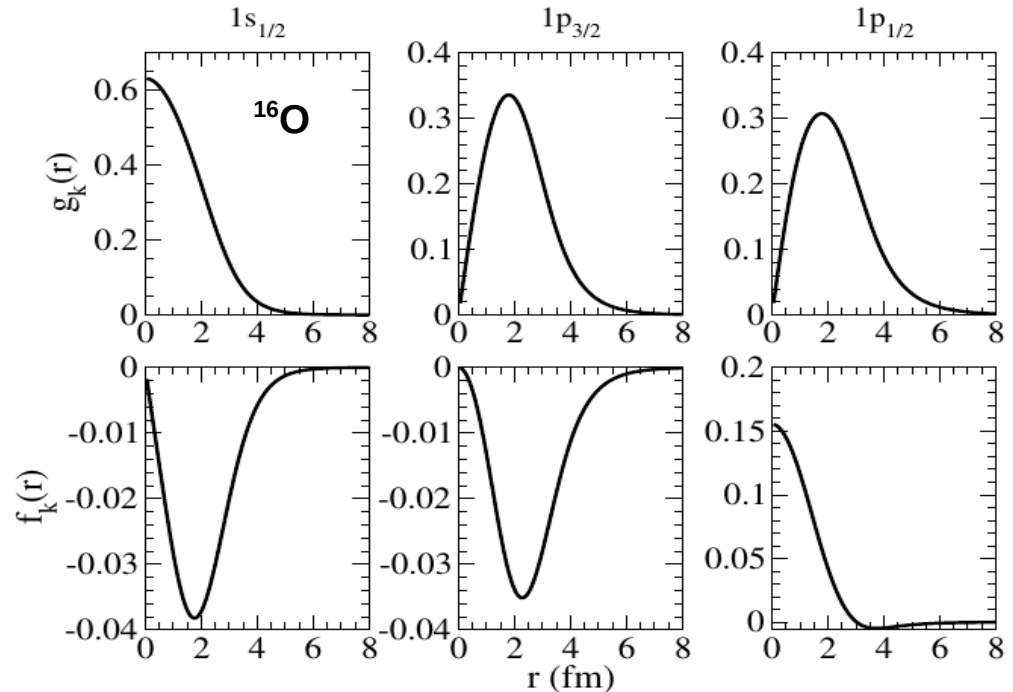
M_N	m_σ	m_ω	m_ρ	g_σ	g_ω	g_ρ	g_2	g_3
939.0	526.059	783.0	763.0	10.444	12.945	4.3830	-6.9099	-15.8337

6 free parameters

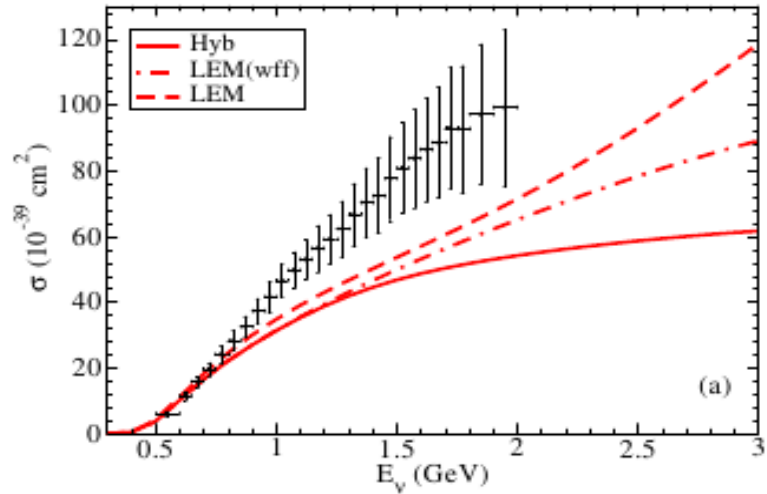
$$[-i\boldsymbol{\alpha} \cdot \boldsymbol{\nabla} + V(r) + \beta(M + S(r))]\Psi_i(\mathbf{r}) = E_i\Psi_i(\mathbf{r})$$

$$\Psi_k^{m_j}(\mathbf{r}) = \begin{pmatrix} g_k(r)\varphi_k^{m_j}(\Omega_r) \\ if_k(r)\varphi_{-k}^{m_j}(\Omega_r) \end{pmatrix},$$

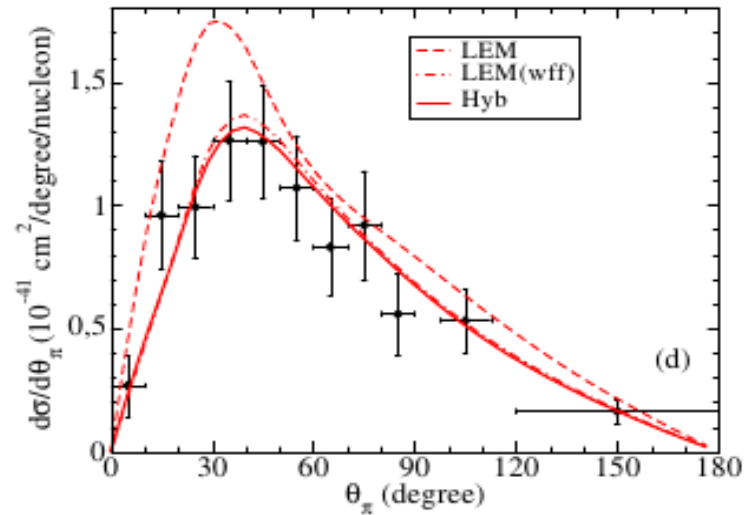
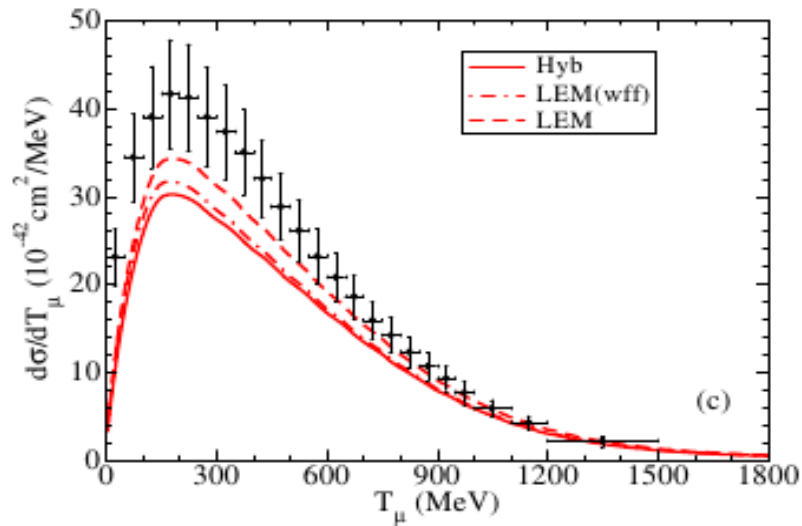
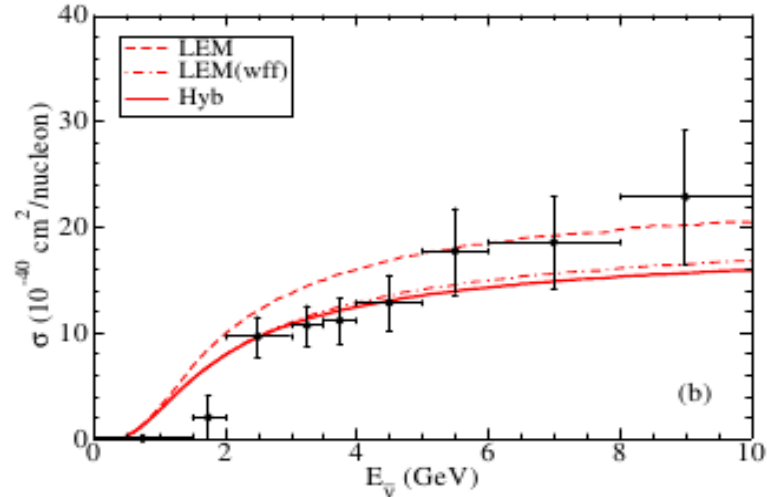
$$\varphi_k^{m_j}(\Omega_r) = \sum_{m_\ell s} \langle \ell m_\ell \frac{1}{2} s | j m_j \rangle Y_\ell^{m_\ell}(\Omega_r) \chi^s$$



MiniBooNE neutrino CC 1pion+.

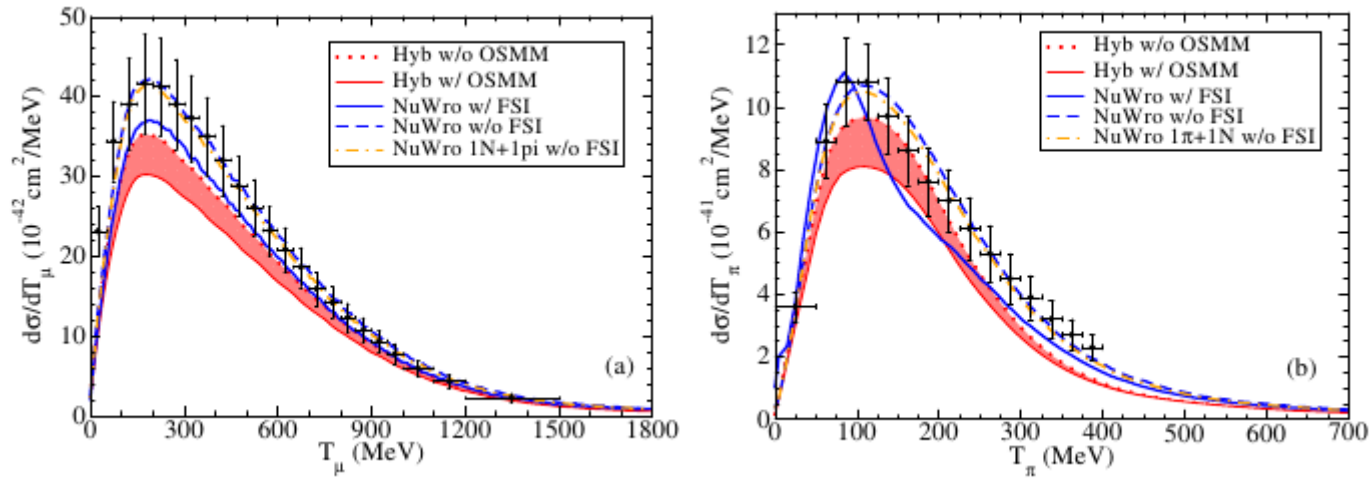


MINERvA antineutrino CC 1pion0.

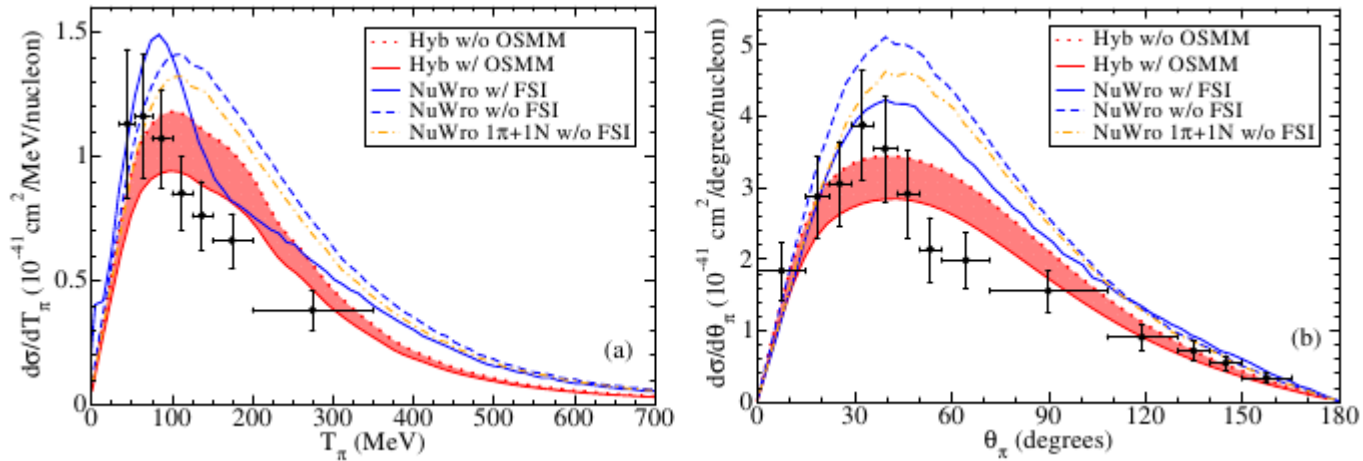


RGJ et al., arXiv:1710.08374 [nucl-th]

MiniBooNE neutrino CC 1pion+.

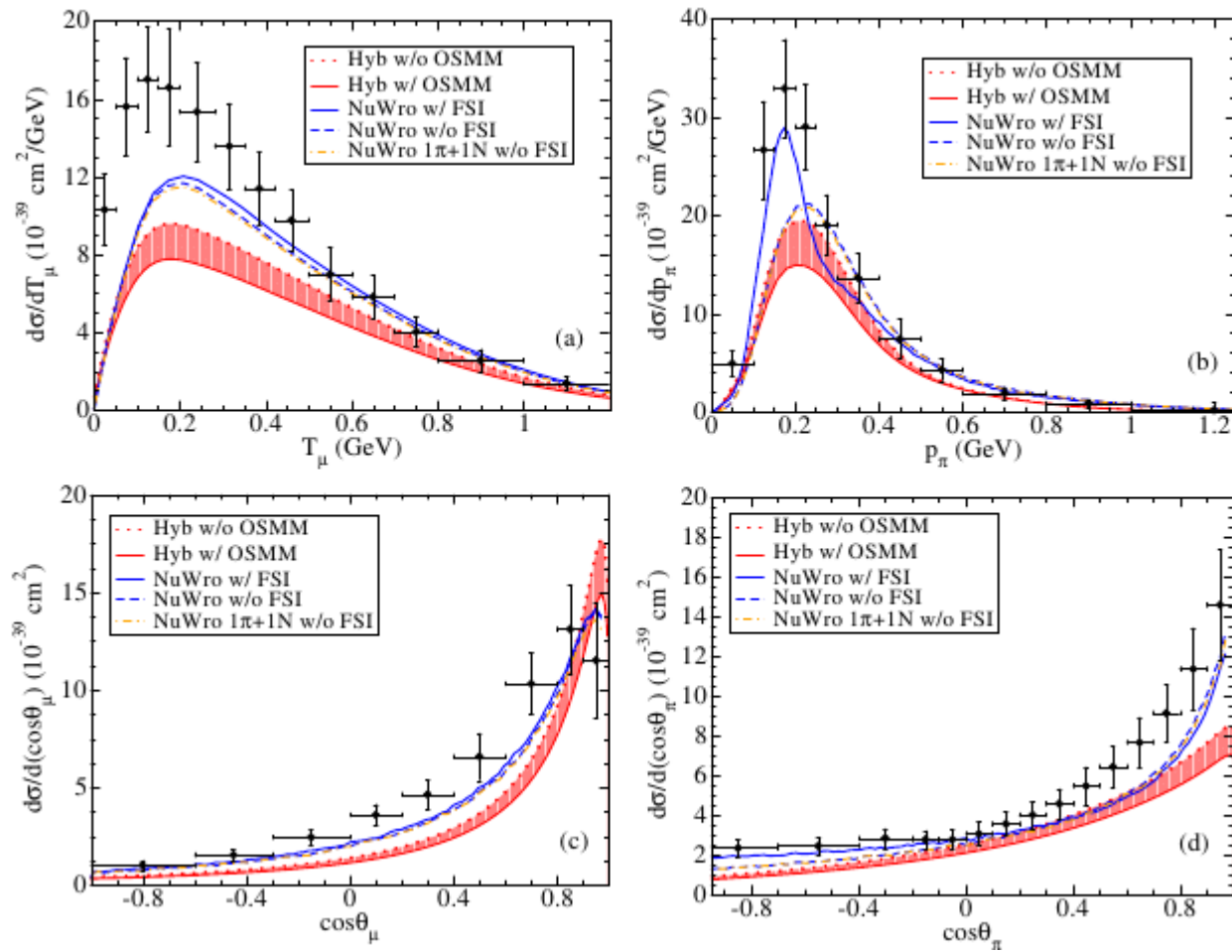


MINERvA antineutrino CC 1pion0.



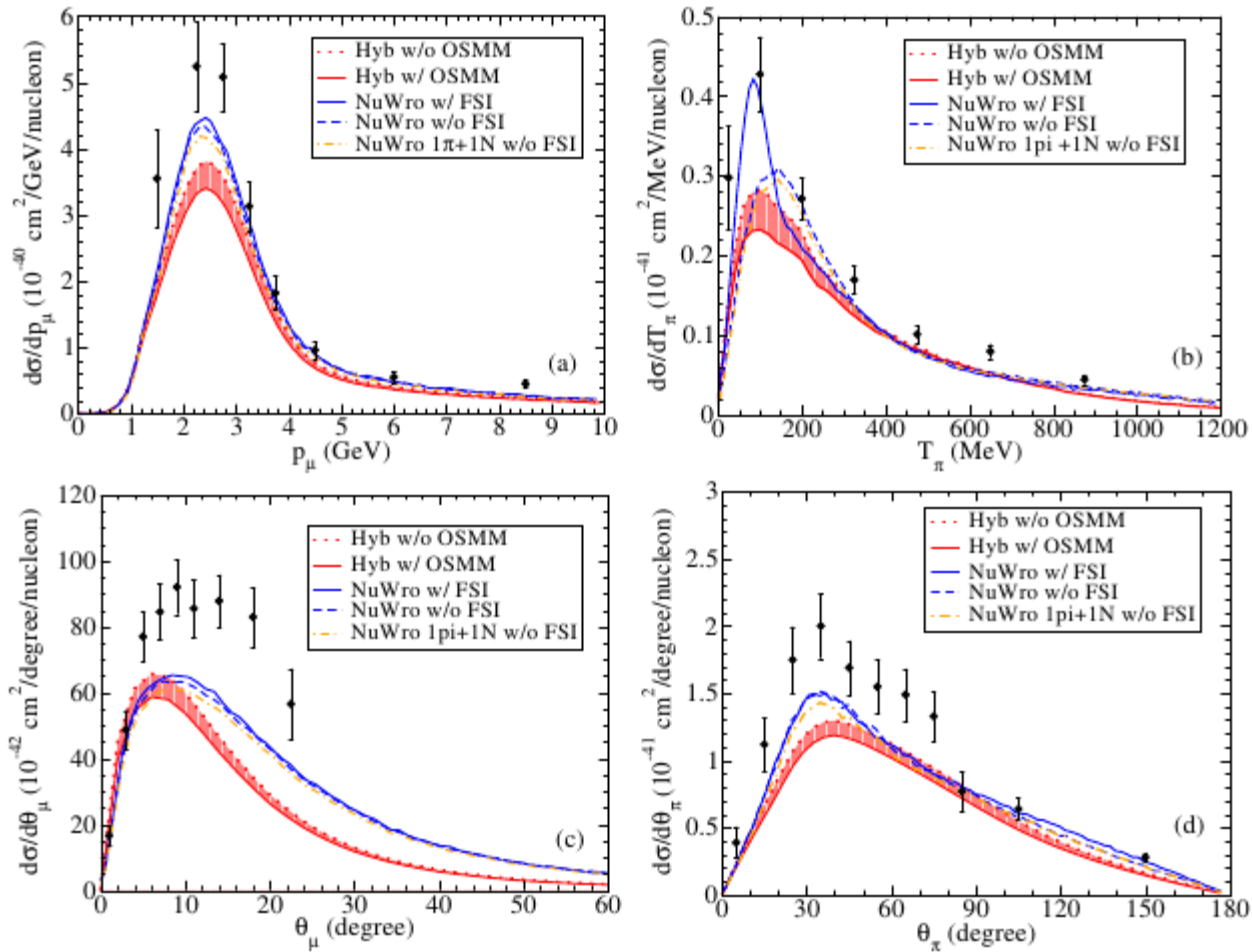
RGJ et al., arXiv:1710.08374 [nucl-th]

MiniBooNE neutrino CC 1pion0.



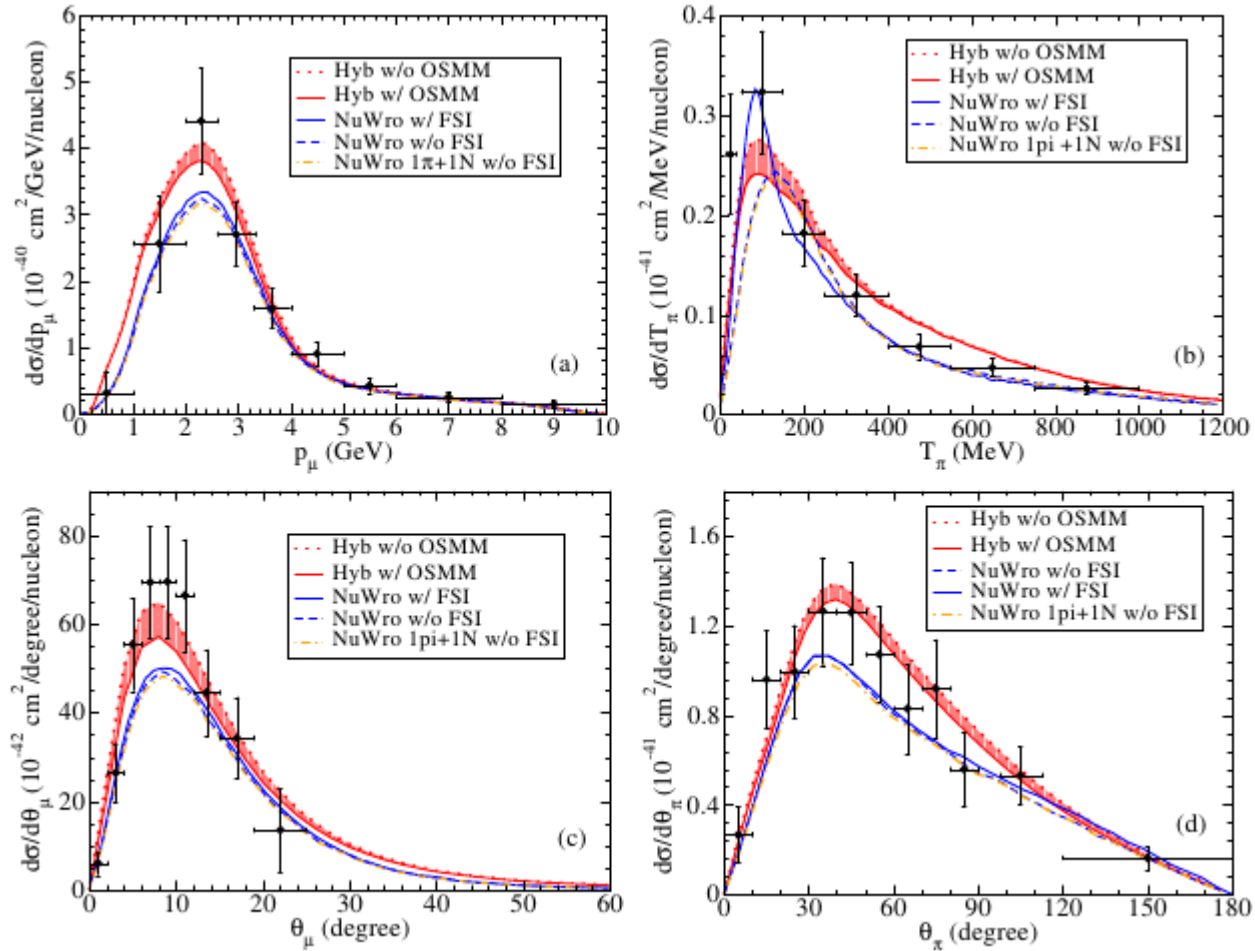
RGJ et al., arXiv:1710.08374 [nucl-th]

MINERvA neutrino CC 1pion0.



RGJ et al., arXiv:1710.08374 [nucl-th]

MINERvA antineutrino CC 1pion0.



RGJ et al., arXiv:1710.08374 [nucl-th]

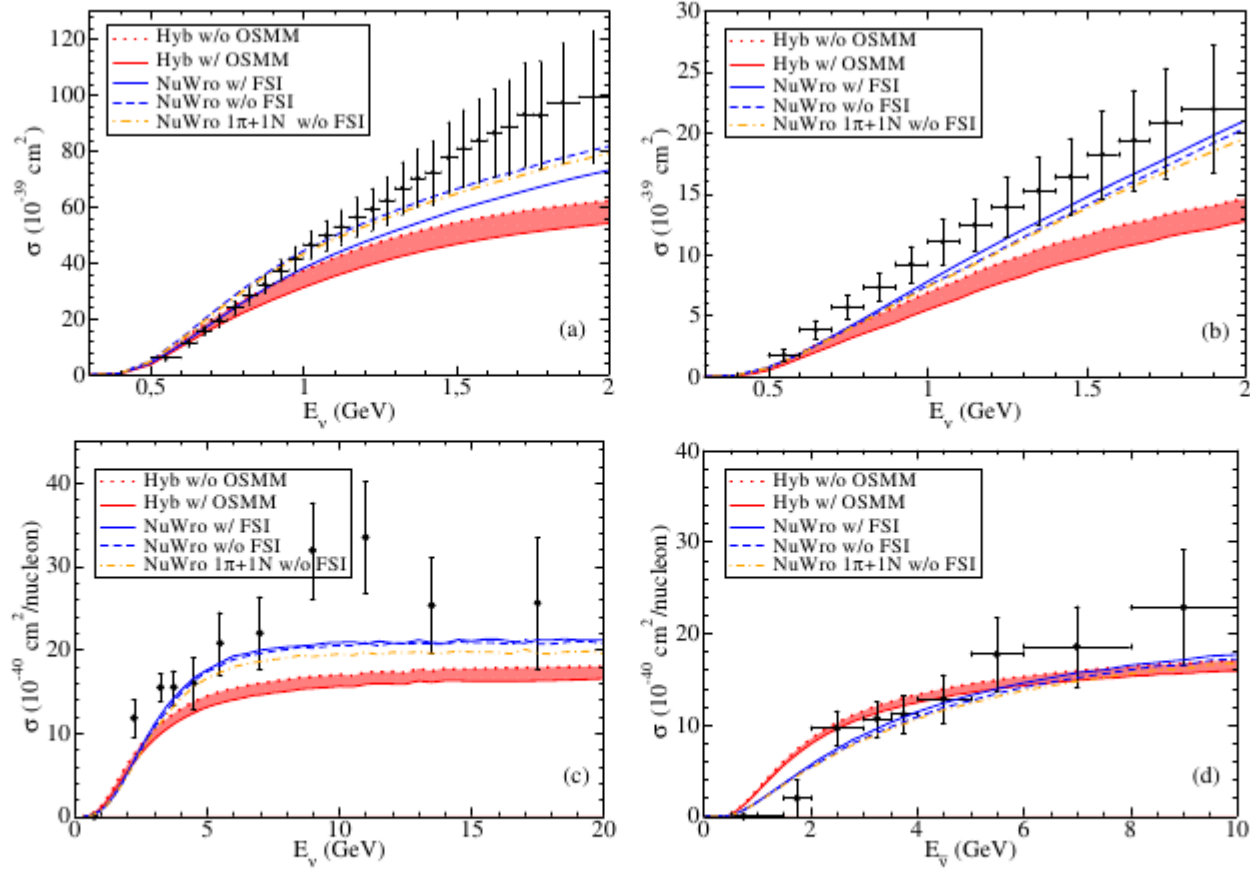


FIG. 10: Total cross section for the reactions (a) MiniBooNE ν CC $1\pi^+$ [4], (b) MiniBooNE ν CC $1\pi^0$ [62], (c) MINERvA ν CC $1\pi^0$ [7], and (d) MINERvA $\bar{\nu}$ CC $1\pi^0$ [6]. Labels as in Fig. 5

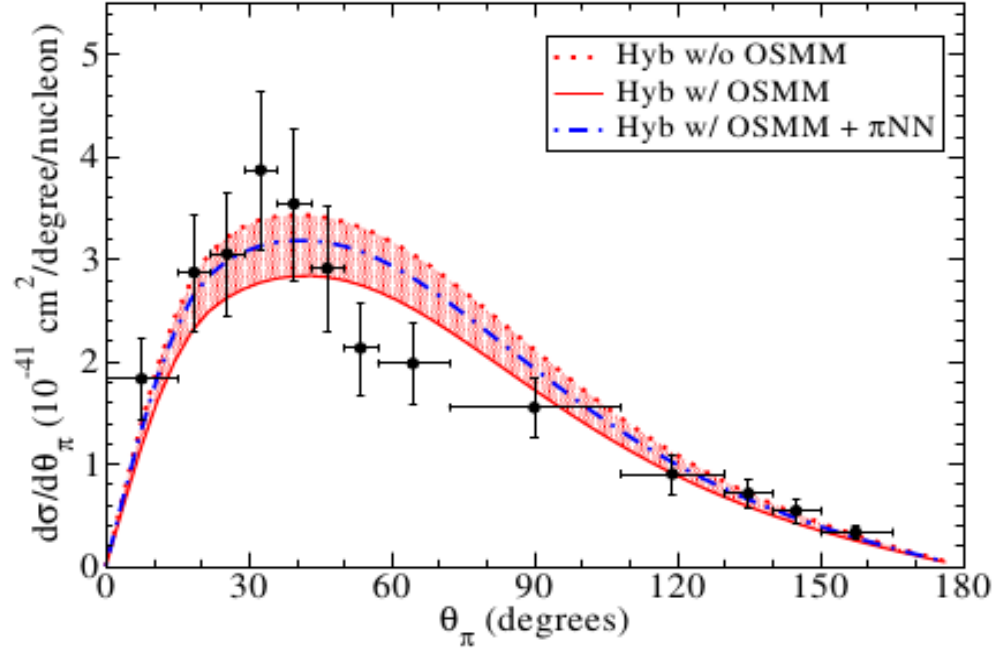


FIG. 3: MINERvA ν -induced $1\pi^+$ production sample [5] compared with RPWIA predictions. Solid (dotted) line is the result with (without) medium modification of the Delta width. The dash-dotted line is the result with OSMM when the contribution from the $\Delta N \rightarrow \pi NN$ channel is added to the cross section. The results were computed with the Hybrid model (see Sec IV B).

Conclusions

- ✓ Simple analysis of the **kinematics of the problem** tell us the minimum set of independent variables that is needed to describe the scattering process.
 - ➔ If in our model we have less than that, we are missing something. Is it important?
- ✓ Is it possible to implement (complex) microscopic models with full kinematics in the MC event generators?
 - ➔ Is it worthy? Are you interested?



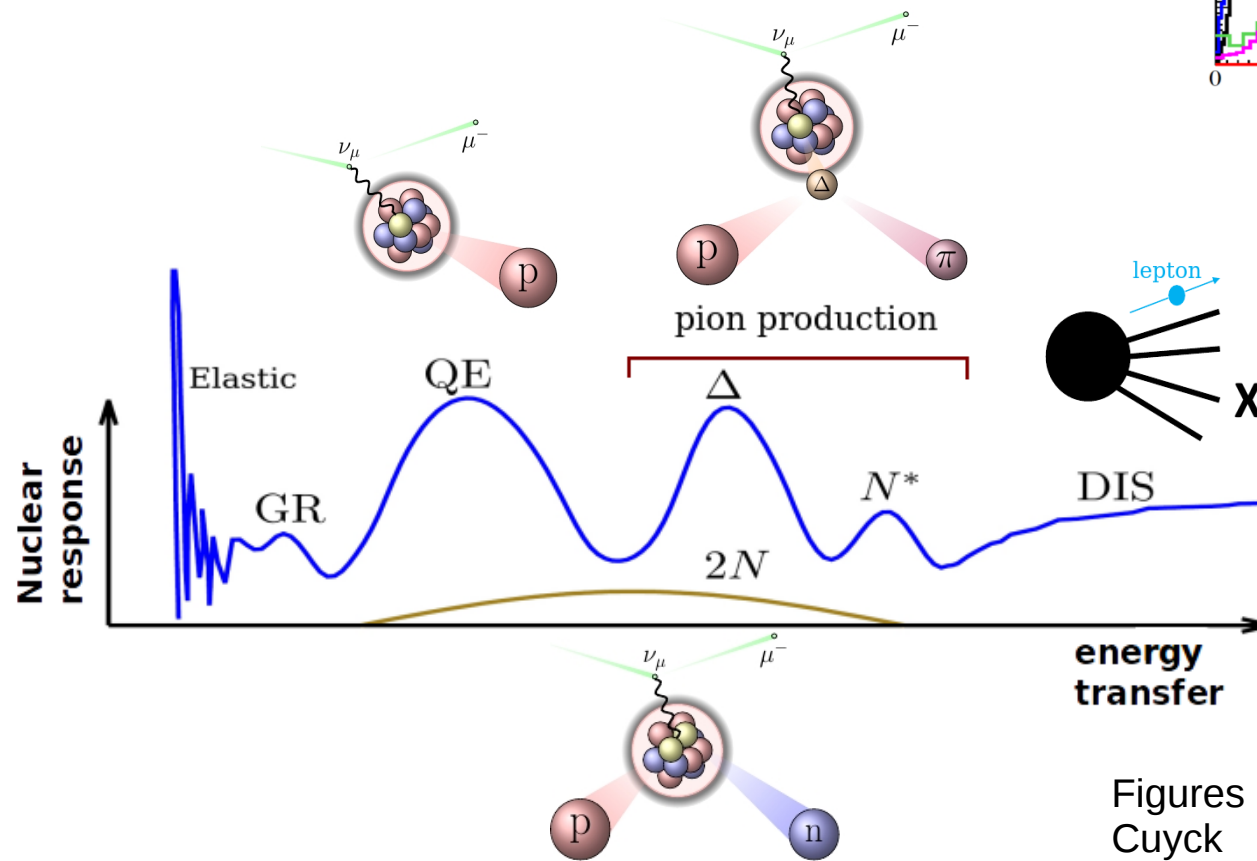
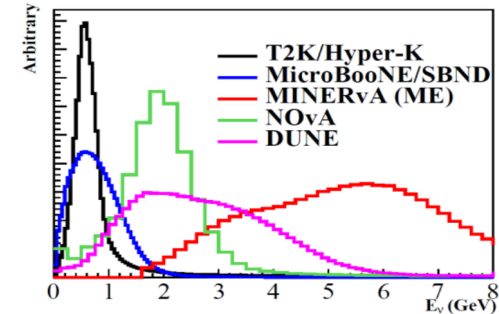
Thanks for your attention

Ghent

Backup slides

What we know from (e,e')

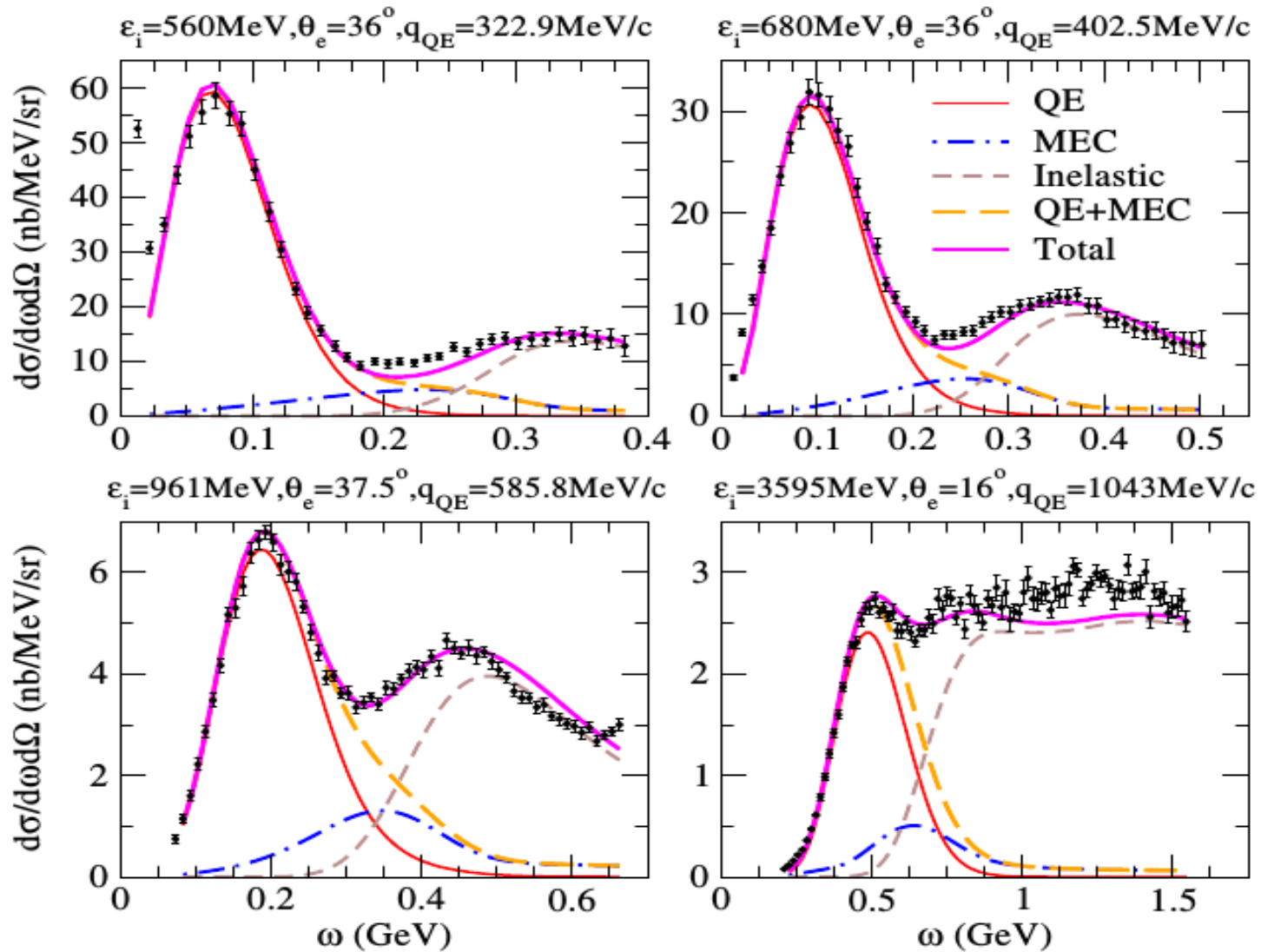
One needs to model all neutrino-nucleus reaction channels covered by the neutrino beam



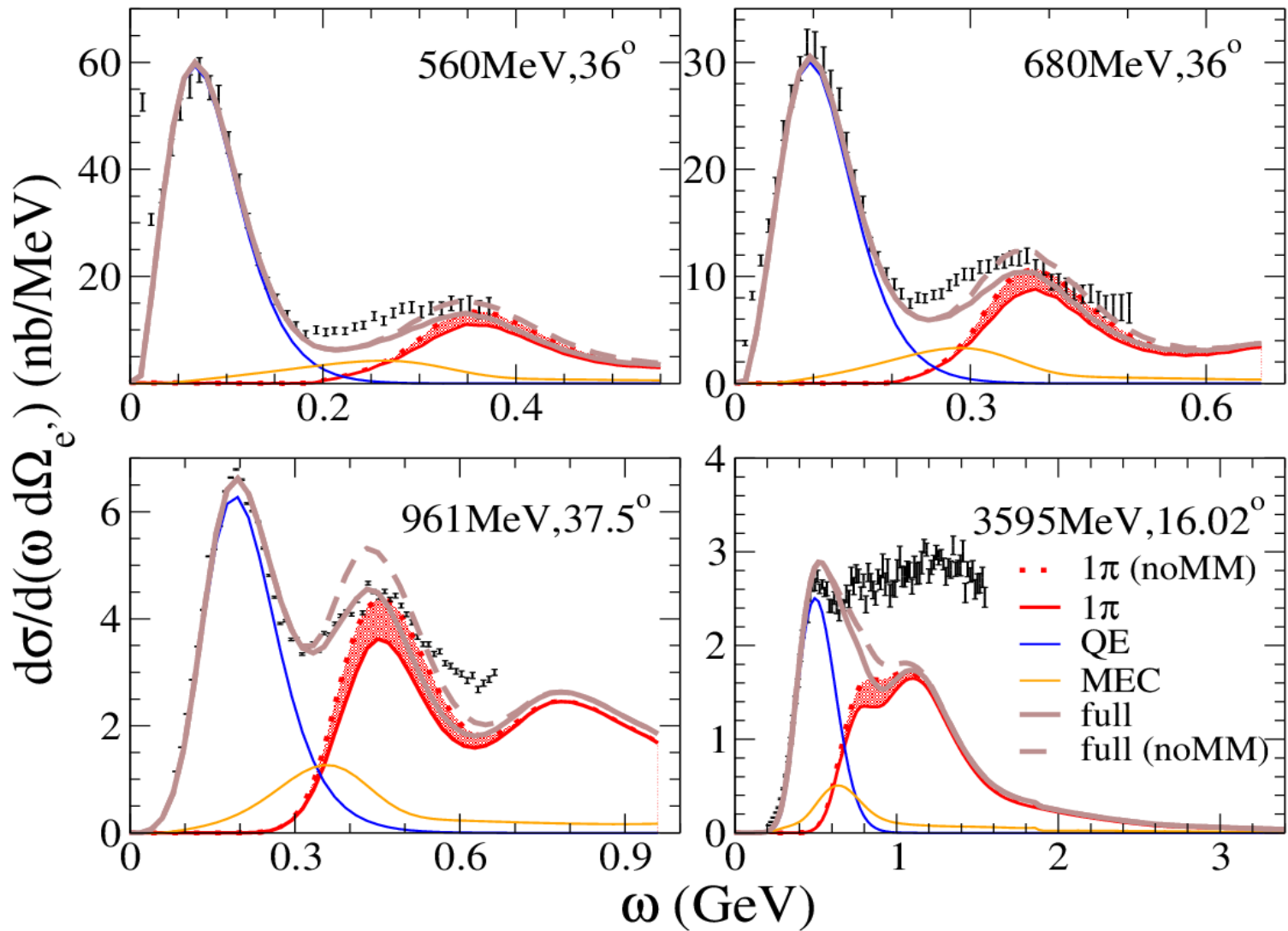
Figures by T. Van Cuyck

What we know from (e,e')

Superscaling approach (Megias et al., Phys. Rev. D 91, 073004 (2015))



What we know from (e,e')



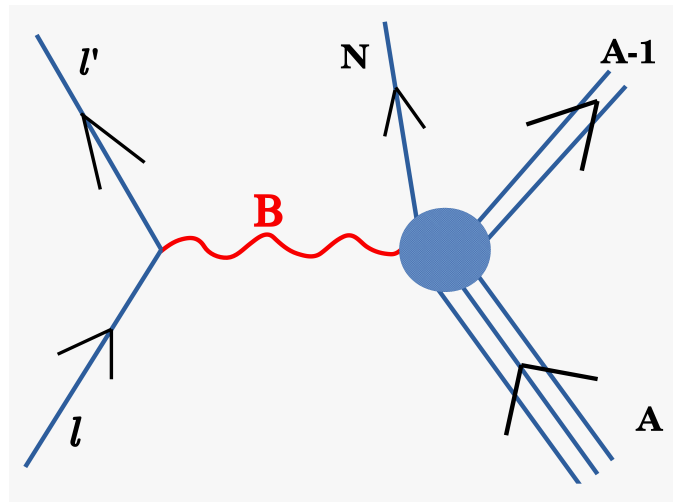
$^{12}\text{C}(e,e')$

QE (SuSAv2):
RGJ et al., PRC 90,
035501 (2014)

MEC: Megias et al.,
PRD 91, 073004
(2015)

1pion: RGJ et al.,
PRD 95, 113007
(2017);
arXiv:1710.08374

Quasielastic scattering



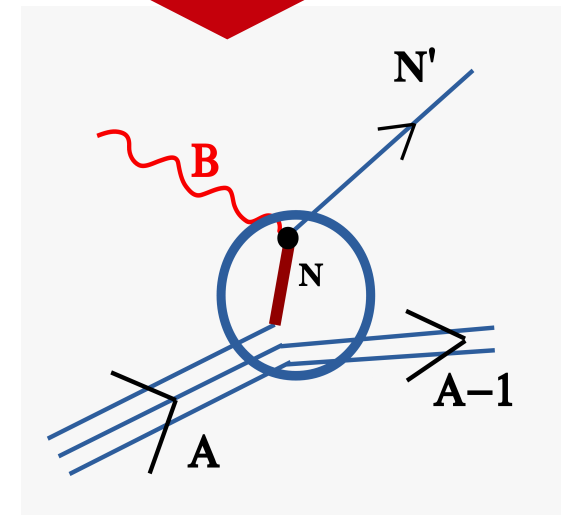
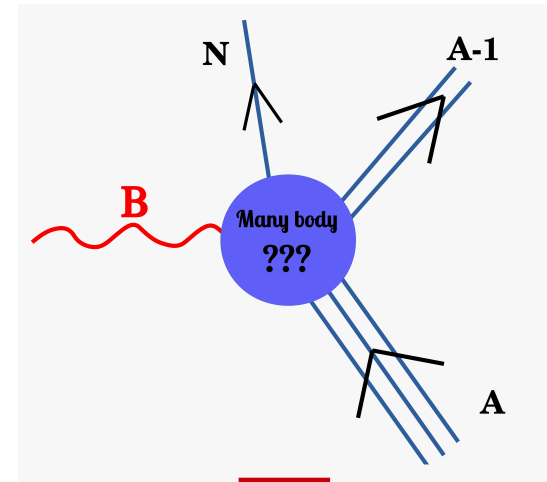
Impulse approximation

$$J_{had}^{\mu} = \langle N, A - 1 | \hat{O}_{many-body}^{\mu} | A \rangle$$

**Impulse
Approximation**

$$J_{had}^{\mu} = \sum_i^A \int dr \bar{\Psi}_F(\mathbf{r}) \hat{O}_{one-body}^{\mu} \Psi_B(\mathbf{r}) e^{i\mathbf{q}\cdot\mathbf{r}}$$

where
$$\hat{O}_{one-body}^{\mu} = F_1 \gamma^{\mu} + i \frac{F_2}{2M_N} \sigma^{\mu\alpha} Q_{\alpha}$$



Impulse approximation

$$J_{had}^{\mu} = \langle N, A - 1 | \hat{O}_{many-body}^{\mu} | A \rangle$$

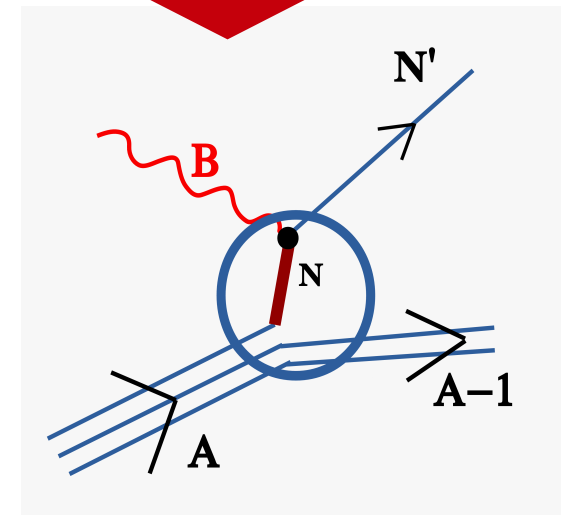
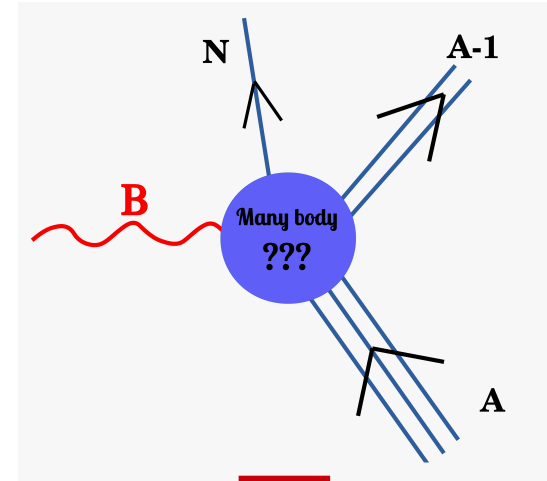
Impulse Approximation

Relativistic mean-field wave functions

$$J_{had}^{\mu} = \sum_i^A \int dr \bar{\Psi}_F(\mathbf{r}) \hat{O}_{one-body}^{\mu} \Psi_B(\mathbf{r}) e^{i\mathbf{q}\cdot\mathbf{r}}$$

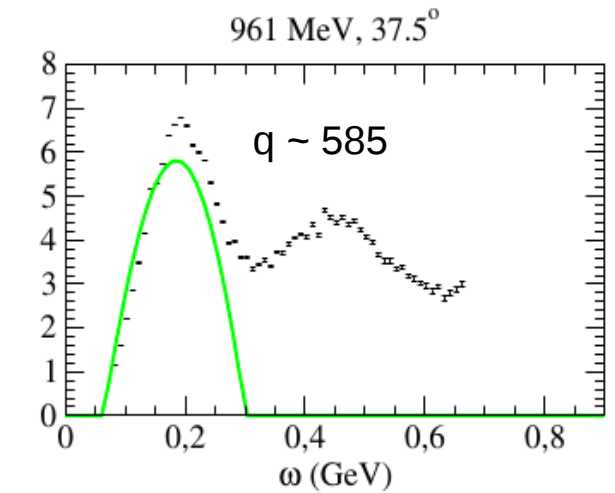
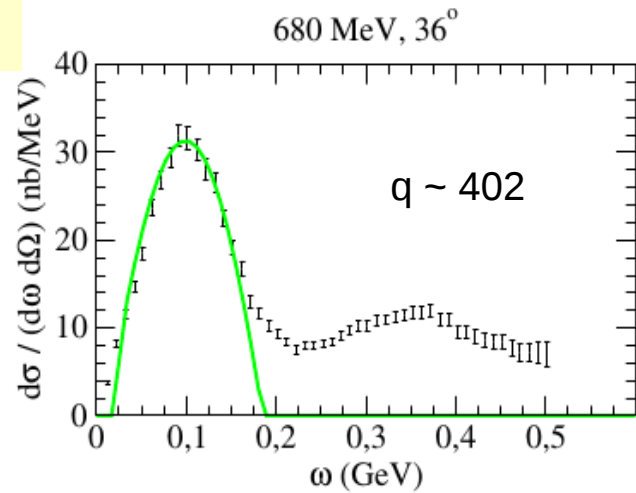
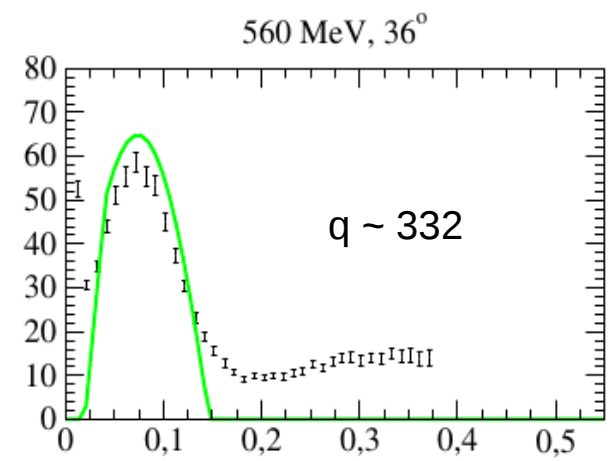
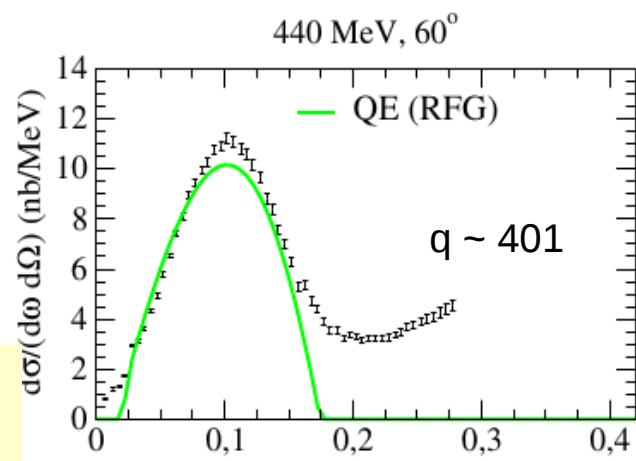
where

$$\hat{O}_{one-body}^{\mu} = F_1 \gamma^{\mu} + i \frac{F_2}{2M_N} \sigma^{\mu\alpha} Q_{\alpha}$$

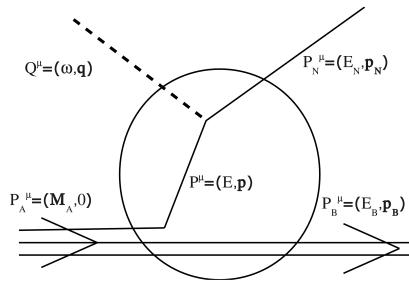


Mean-field vs plane waves

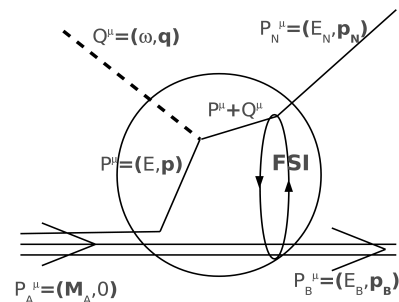
Intermediate energies (typical QE regime)



Mean-field vs plane waves



RPWIA: Scattered nucleon wf is described as a Dirac plane wave.

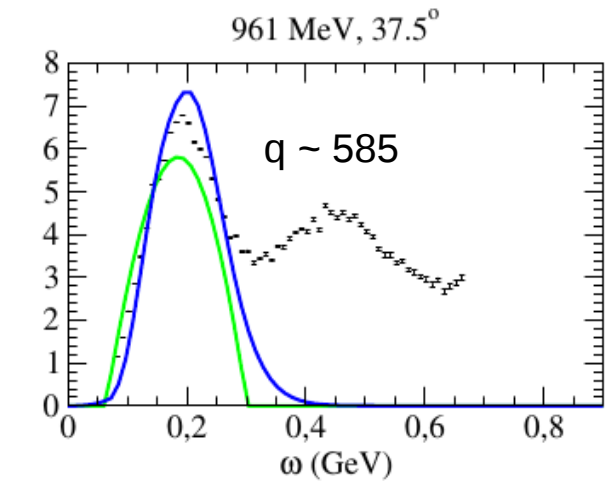
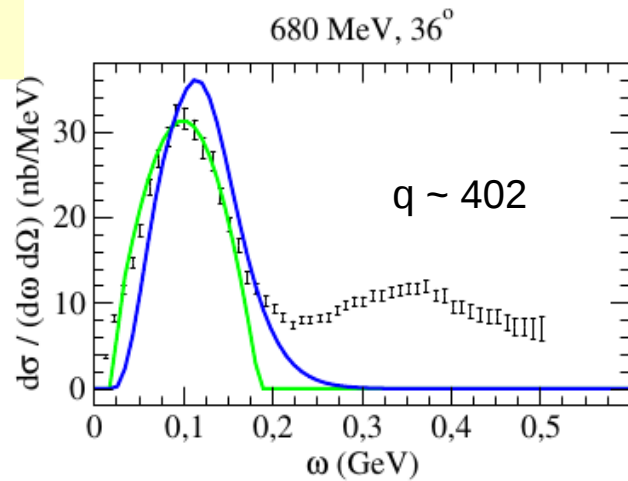
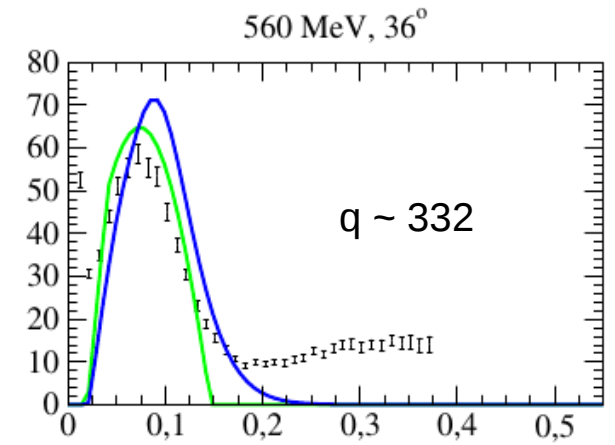
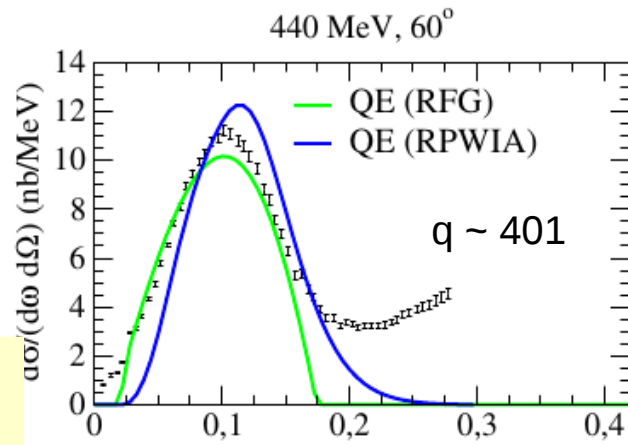


RMF-FSI: Scattered nucleon wf is solution of Dirac eq. in presence of the same potentials used to describe the bound nucleon wf.

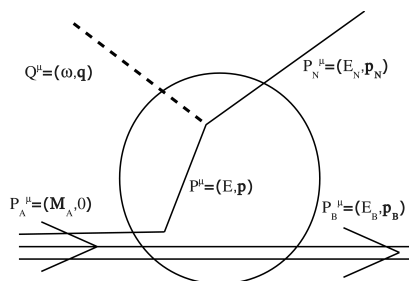
$$[-i\alpha \cdot \nabla + V(r) + \beta(M + S(r))]\Psi_i(\mathbf{r}) = E_i\Psi_i(\mathbf{r})$$

$$J_{had}^\mu = \sum_i^A \int d\mathbf{r} \bar{\Psi}_F(\mathbf{r}) \hat{O}_{one-body}^\mu \Psi_B(\mathbf{r}) e^{i\mathbf{q}\cdot\mathbf{r}}$$

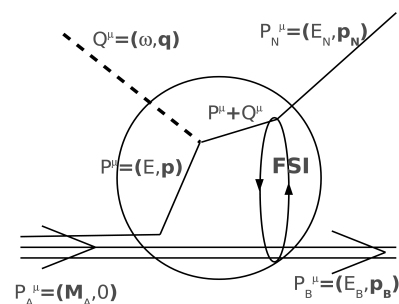
Intermediate energies (typical QE regime)



Mean-field vs plane waves



RPWIA: Scattered nucleon wf is described as a Dirac plane wave.

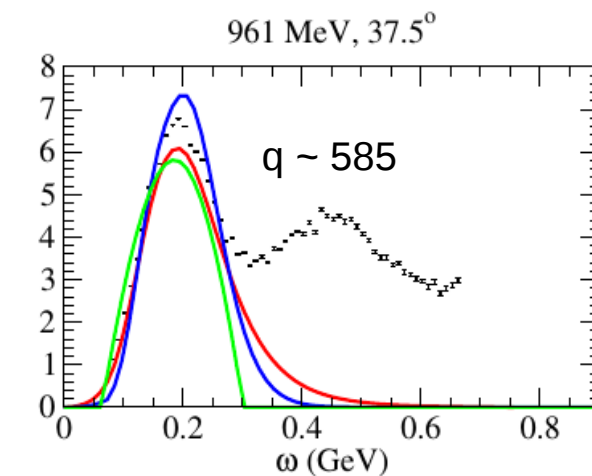
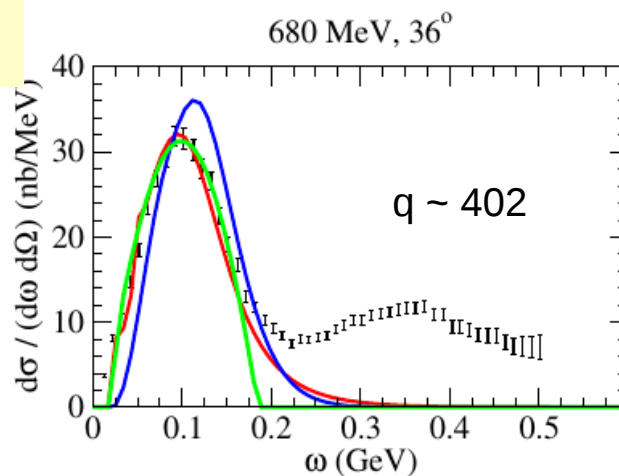
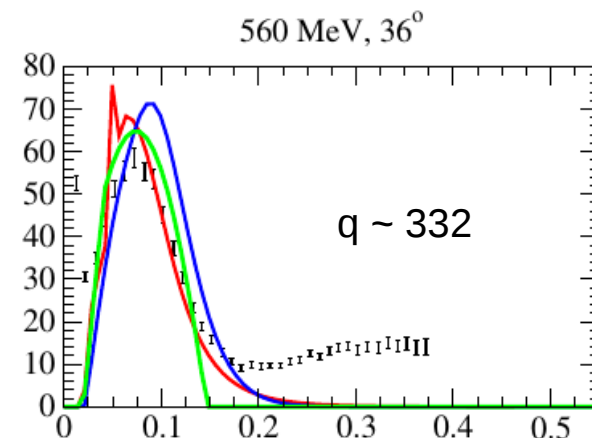
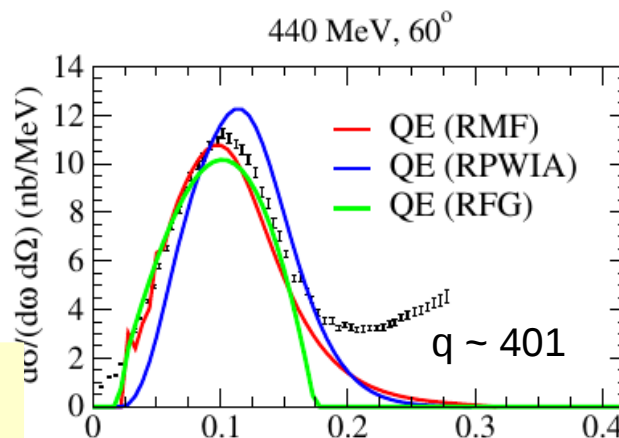


RMF-FSI: Scattered nucleon wf is solution of Dirac eq. in presence of the same potentials used to describe the bound nucleon wf.

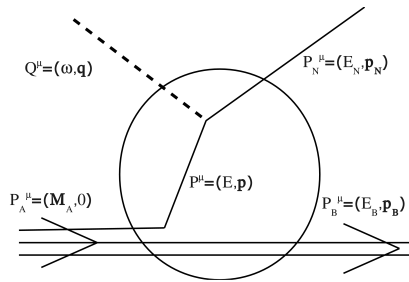
$$[-i\alpha \cdot \nabla + V(r) + \beta(M + S(r))]\Psi_i(\mathbf{r}) = E_i\Psi_i(\mathbf{r})$$

$$J_{had}^\mu = \sum_i^A \int d\mathbf{r} \bar{\Psi}_F(\mathbf{r}) \hat{O}_{one-body}^\mu \Psi_B(\mathbf{r}) e^{i\mathbf{q}\cdot\mathbf{r}}$$

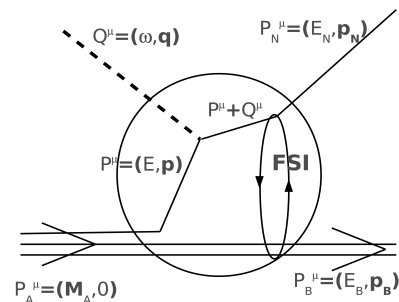
Intermediate energies (typical QE regime)



Mean-field vs plane waves



RPWIA: Scattered nucleon wf is described as a Dirac plane wave.

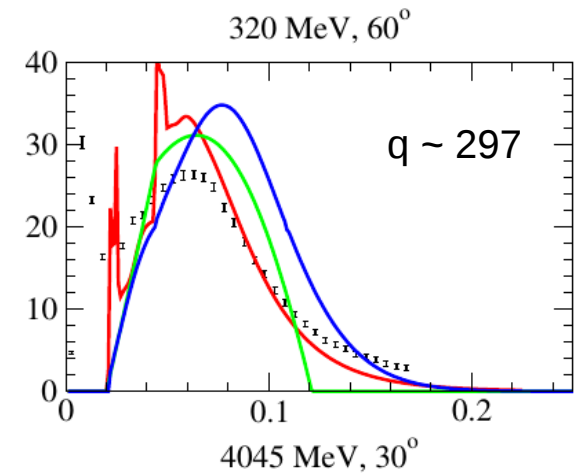
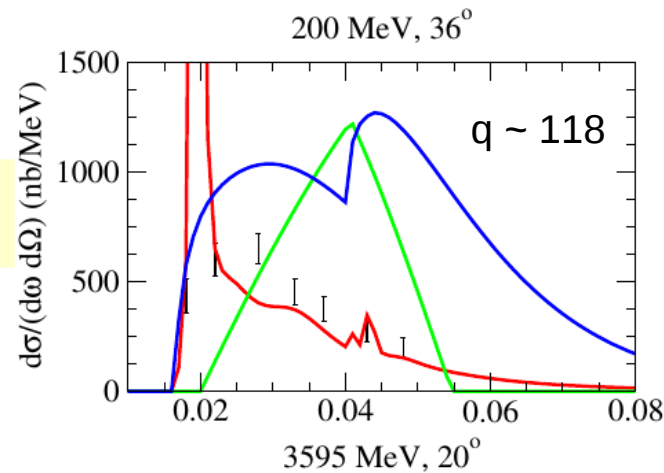


RMF-FSI: Scattered nucleon wf is solution of Dirac eq. in presence of the same potentials used to describe the bound nucleon wf.

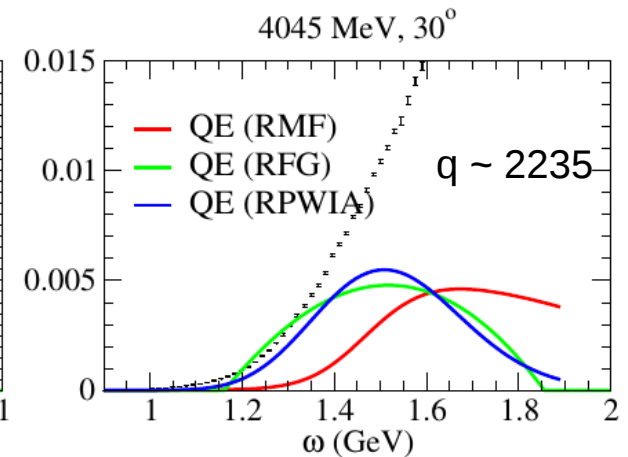
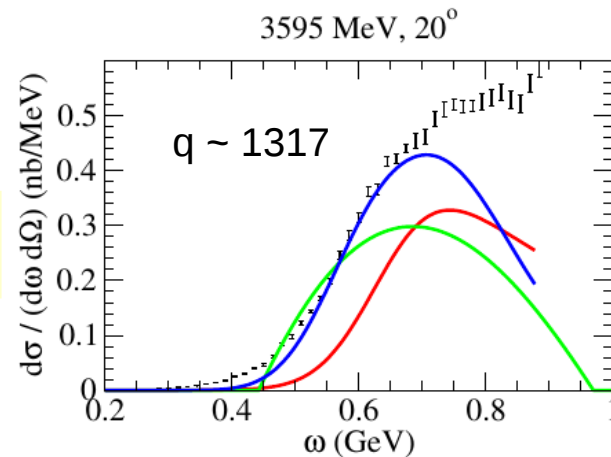
$$[-i\alpha \cdot \nabla + V(r) + \beta(M + S(r))]\Psi_i(\mathbf{r}) = E_i\Psi_i(\mathbf{r})$$

$$J_{had}^\mu = \sum_i^A \int d\mathbf{r} \bar{\Psi}_F(\mathbf{r}) \hat{O}_{one-body}^\mu \Psi_B(\mathbf{r}) e^{i\mathbf{q}\cdot\mathbf{r}}$$

Low energies



High energies



Back slides: isospin coefficients and resonances parameters

Channel	ΔP	$C\Delta P$	NP	CNP	Others
$p \rightarrow \pi^+ + p$	$\sqrt{3/2}$	$\sqrt{1/6}$	0	1	1
$n \rightarrow \pi^0 + p$	$-\sqrt{1/3}$	$\sqrt{1/3}$	$\sqrt{1/2}$	$-\sqrt{1/2}$	$-\sqrt{2}$
$n \rightarrow \pi^+ + n$	$\sqrt{1/6}$	$\sqrt{3/2}$	1	0	-1
$n \rightarrow \pi^- + n$	$\sqrt{3/2}$	$\sqrt{1/6}$	0	1	1
$p \rightarrow \pi^0 + n$	$\sqrt{1/3}$	$-\sqrt{1/3}$	$-\sqrt{1/2}$	$\sqrt{1/2}$	$\sqrt{2}$
$p \rightarrow \pi^- + p$	$\sqrt{1/6}$	$\sqrt{3/2}$	1	0	-1

Table: Isospin coefficients for the CC reaction.

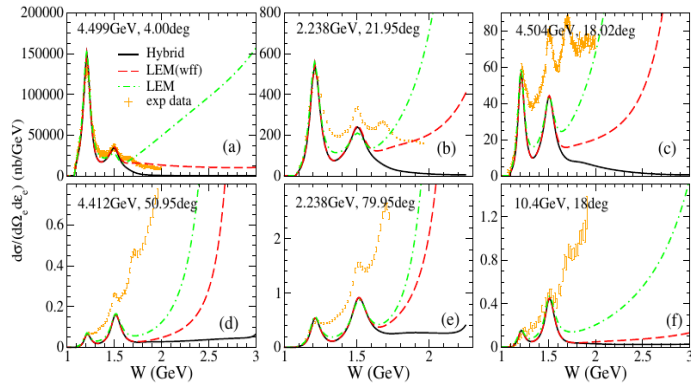
Channel	ΔP	$C\Delta P$	NP	CNP	Others
$p \rightarrow \pi^0 + p$	$\sqrt{1/3}$	$\sqrt{1/3}$	$\sqrt{1/2}$	$\sqrt{1/2}$	0
$p \rightarrow \pi^+ + n$	$-\sqrt{1/6}$	$\sqrt{1/6}$	1	1	-1
$n \rightarrow \pi^- + p$	$\sqrt{1/6}$	$-\sqrt{1/6}$	1	1	1
$n \rightarrow \pi^0 + n$	$\sqrt{1/3}$	$\sqrt{1/3}$	$-\sqrt{1/2}$	$-\sqrt{1/2}$	0

Table: Isospin coefficients for the neutral current (EM and WNC) reactions.

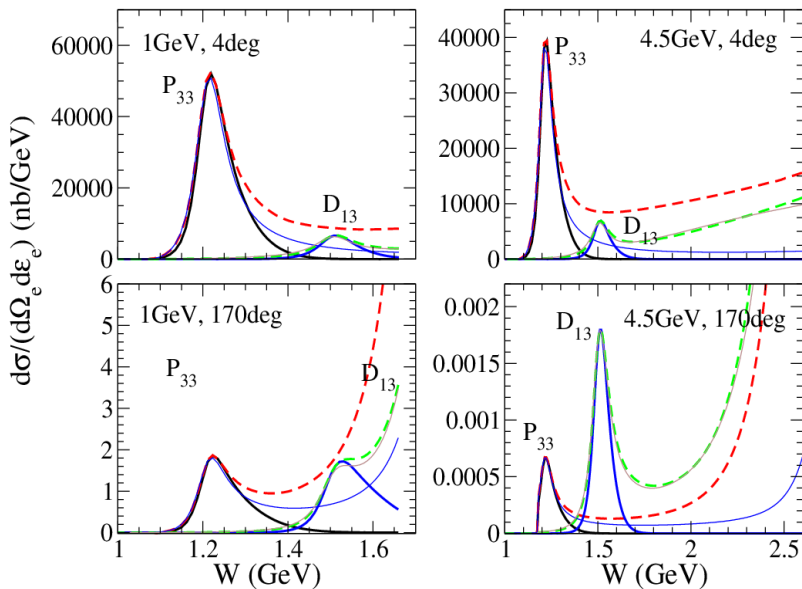
	I	S	P	M_R	πN -br	$\Gamma_{\text{width}}^{\text{exp}}$	$f_{\pi NR}$
P_{33}	3/2	3/2	+	1232	100%	120	2.18
D_{13}	1/2	3/2	-	1515	60%	115	1.62
P_{11}	1/2	1/2	+	1430	65%	350	0.391
S_{11}	1/2	1/2	-	1535	45%	150	0.16

Table: quantum numbers and other parameters of the nucleon resonances.

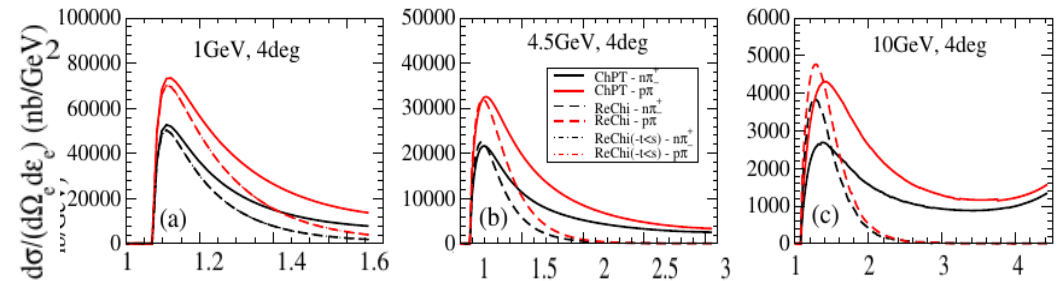
The Problem



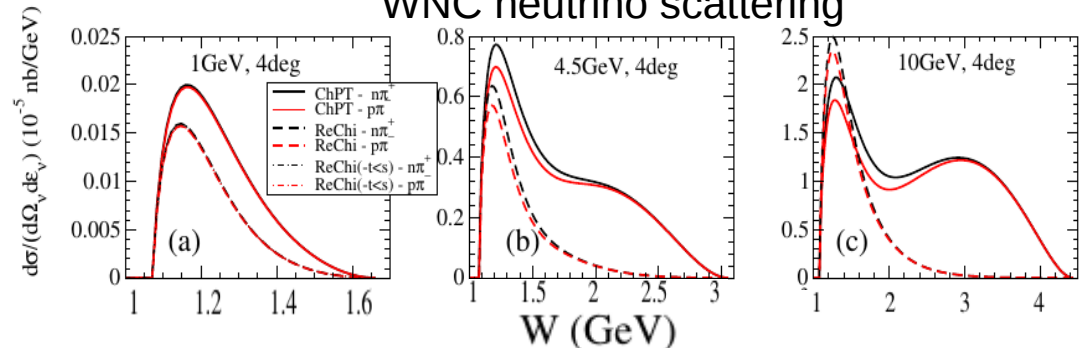
The pathologies come from the **resonances** and **background terms**



Electron scattering

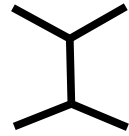


WNC neutrino scattering



Why does this happen?

Cross channels:



$$\mathcal{A}(t, s) = \sum_{\ell} (2\ell + 1) A_{\ell}(t) P_{\ell}(z_t)$$

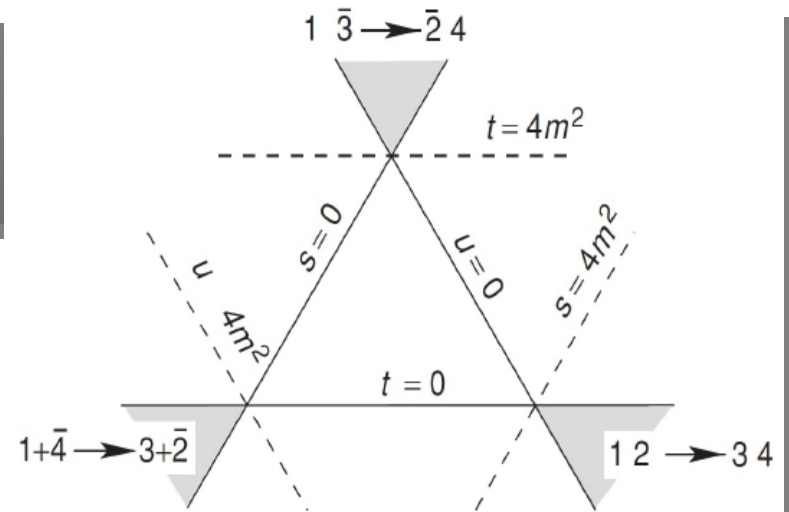
$$P_{\ell}(z_t) \xrightarrow{s \rightarrow \infty} (2s)^{\ell}$$

Direct channels:



$$\mathcal{A}(s, t) = \sum_{\ell} (2\ell + 1) A_{\ell}(s) P_{\ell}(z_s)$$

$$A_{\ell}(s) \sim \left(\frac{s - 4m^2}{2} \right)^{\ell}$$



$$z_t \equiv \cos \theta_t = 1 + \frac{2s}{t - 4m^2}$$

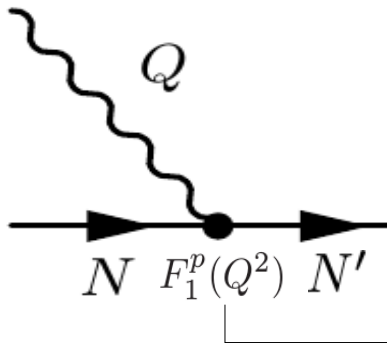
$$z_s \equiv \cos \theta_s = 1 + \frac{2t}{s - 4m^2}$$

Behavior at threshold (barrier factor).
Feynman diagrams provide the right behavior at threshold but not at high s

High-energy model

Regge approach for the vector amplitudes.

We use the approach first proposed by **Kaskulov and Mosel** [PRC81, 045202 (2010)] to extends GLV to the case of pion electroproduction ($Q^2 \neq 0$).



The nucleon N' may be highly off its mass shell.

Therefore, instead of using the on shell form factor $F_1^p(Q^2)$.

We use a form factor that accounts for the off shell character of the nucleon [**Vrancx and Ryckebusch**, PRC89, 025203 (2014)]:

$$F_1^p(Q^2, s) = \left(1 + \frac{Q^2}{\Lambda_{\gamma pp^*}(s)^2} \right)^{-2}$$

$$\Lambda_{\gamma pp^*}(s) = \Lambda_{\gamma pp} + (\Lambda_{\infty} - \Lambda_{\gamma pp}) \left(1 - \frac{M^2}{s} \right)$$

$$\Lambda_{\infty} = 2.194 \text{ GeV}$$

In the (on shell) limit the Dirac form factor is recovered.

High-energy model

“Reggeizing” the ChPT background:

$$\mathcal{O}_{ReChi,V}^\mu = \mathcal{O}_{ChPT,V}^\mu \mathcal{P}_\pi(t, s)(t - m_\pi^2)$$

high-energy model:
ReChi (from Reggeized
ChPT background)

low-energy model (only
the ChPT background)

The pion propagator is replaced
by the **Regge propagator** of the
pion trajectory

$$\mathcal{O}_{ReChi,A}^\mu = \mathcal{O}_{ChPT,A}^\mu \mathcal{P}_\rho(t, s)(t - m_\rho^2)$$

Regge Theory

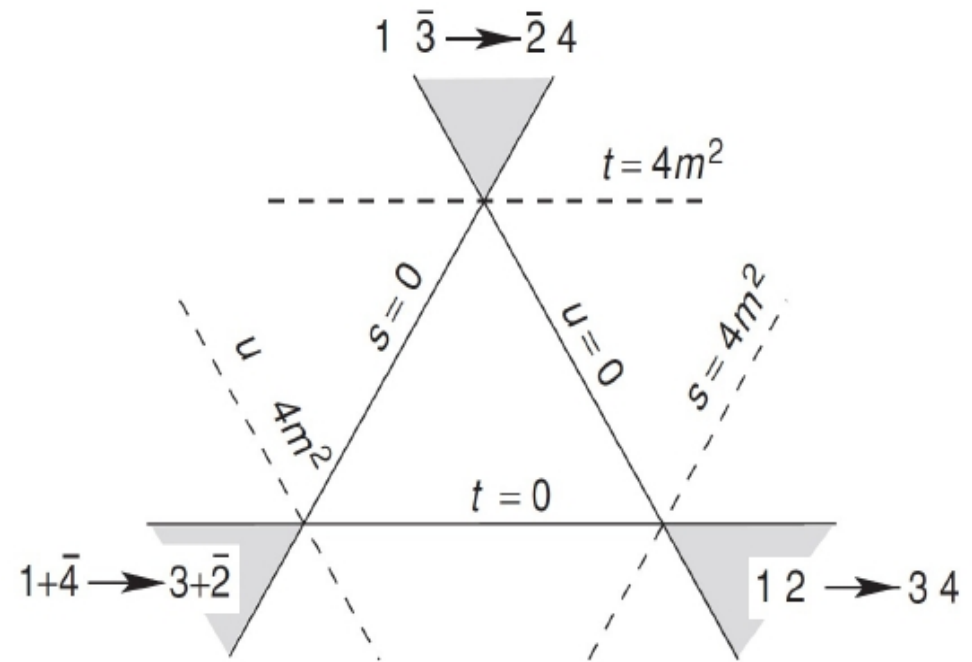
$$A(t, s) = \sum_{\ell} (2\ell + 1) A_{\ell}(t) P_{\ell}(z_t)$$

$$z_t \equiv \cos \theta_t = 1 + \frac{2s}{t - 4m^2}$$

$$L=0 \quad + \quad L=1 \quad + \quad \dots$$

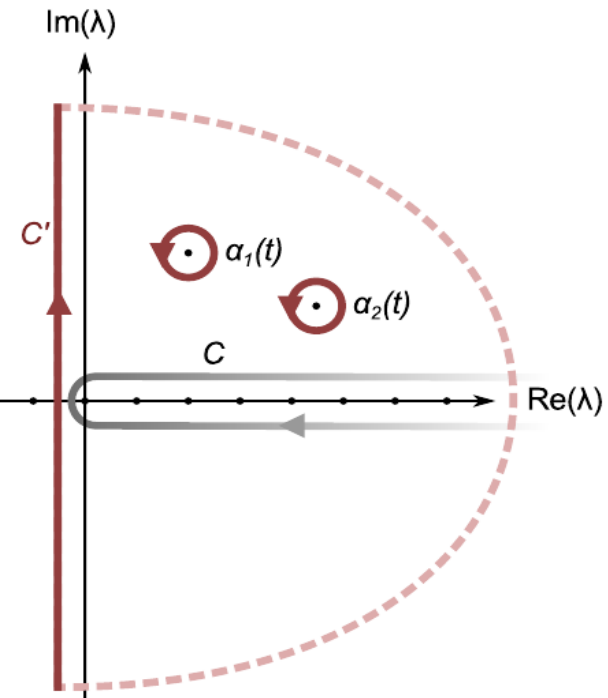
$$\frac{\lambda^2}{m^2 - t}$$

$$P_{\ell}(z_t) \xrightarrow{s \rightarrow \infty} (2s)^{\ell}$$



Regge Theory

$$\mathcal{M}(s, t) = -\frac{1}{2i} \oint_{C_1} d\lambda \frac{(2\lambda + 1) \mathcal{M}_\lambda(t) P_\lambda(-\cos \theta_t)}{\sin(\pi\lambda)}$$



$$\mathcal{M}_{\text{Regge}}^\zeta(s, t) = C \sum_i \left(\frac{s}{s_0} \right)^{\alpha_i^\zeta(t)} \frac{\beta_i^\zeta(t)}{\sin(\pi\alpha_i^\zeta(t))} \frac{1 + \zeta e^{-i\pi\alpha_i^\zeta(t)}}{2} \frac{1}{\Gamma(\alpha_i^\zeta(t) + 1)}$$

Hybrid model

1) Regularizing the behavior of resonances (u- and s-channel contributions): we multiply the resonance amplitude by a dipole-Gaussian form factor

$$F(s, u) = F(s) + F(u) - F(s)F(u)$$

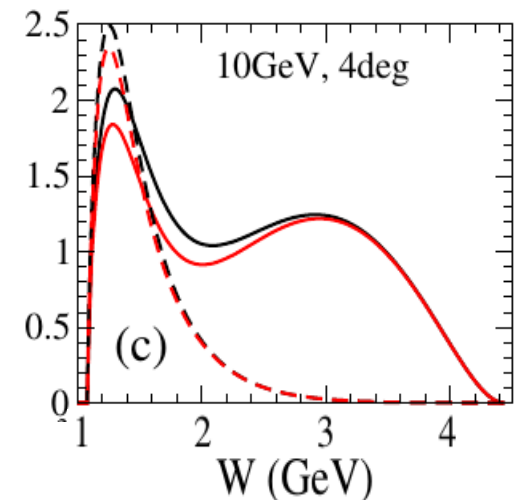
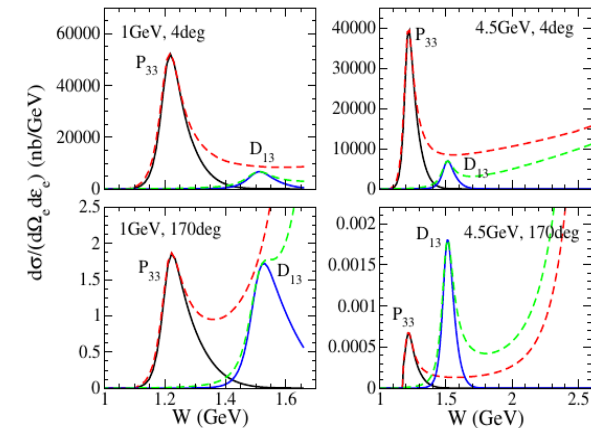
$$F(s) = \exp\left(\frac{-(s - M_R^2)^2}{\lambda_R^4}\right) \frac{\lambda_R^4}{(s - M_R^2)^2 + \lambda_R^4}$$

2) Gradually replacing the ChPT background by the High-energy (ReChi) model: we use a phenomenological transition function

$$\tilde{\mathcal{O}} = \cos^2 \phi(W) \mathcal{O}_{ChPT} + \sin^2 \phi(W) \mathcal{O}_{ReChi}$$

$$\phi(W) = \frac{\pi}{2} \left(1 - \frac{1}{1 + \exp\left[\frac{W - W_0}{L}\right]} \right), \quad W_0 = 1.7 \text{ GeV}$$

$$L = 100 \text{ MeV}$$



Medium modifications of the Delta

Delta propagator:

$$S_{\Delta,\alpha\beta} = \frac{-(K_{\Delta} + M_{\Delta})}{K_{\Delta}^2 - M_{\Delta}^2 + iM_{\Delta}\Gamma_{\text{width}}} \left(g_{\alpha\beta} - \frac{1}{3}\gamma_{\alpha}\gamma_{\beta} - \frac{2}{3M_{\Delta}^2}K_{\Delta,\alpha}K_{\Delta,\beta} - \frac{2}{3M_{\Delta}}(\gamma_{\alpha}K_{\Delta,\beta} - K_{\Delta,\alpha}\gamma_{\beta}) \right)$$

with the energy dependent Delta width:

$$\Gamma_{\text{width}}(W) = \frac{1}{12\pi} \frac{(f_{\pi N\Delta})^2}{m_{\pi}^2 W} (\rho_{\pi,cm})^3 (M + E_{N,cm})$$

$$\Gamma_{\text{width}}^{\text{free}} \longrightarrow \Gamma_{\text{width}}^{\text{in-medium}} = \Gamma_{\text{Pauli}} - 2\Im(\Sigma_{\Delta}), \quad M_{\Delta}^{\text{free}} \longrightarrow M_{\Delta}^{\text{in-medium}} = M_{\Delta}^{\text{free}} + \Re(\Sigma_{\Delta}).$$

+ Γ_{Pauli} : some nucleons from Δ -decay are Pauli blocked (the Δ -decay width decreases).

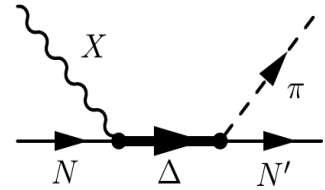
+ The parametrization of $\Im(\Sigma_{\Delta})$ and $\Re(\Sigma_{\Delta})$ is given in terms of the nuclear density ρ :

$$\begin{aligned} -\Im(\Sigma_{\Delta}) &= C_{QE} (\rho/\rho_0)^{\alpha} + C_{A2} (\rho/\rho_0)^{\beta} + C_{A3} (\rho/\rho_0)^{\gamma}, \\ \Re(\Sigma_{\Delta}) &= 40 \text{ MeV} (\rho/\rho_0). \end{aligned}$$

We modify the free $\Delta\pi N$ -decay constant ($f_{\Delta\pi N}$) to take into account the E -dependent medium modification of the Δ width:

$$f_{\Delta\pi N}^{\text{in-medium}}(W) = f_{\Delta\pi N} \sqrt{\frac{\Gamma_{\text{Pauli}} + 2C_{QE} (\rho/\rho_0)^{\alpha}}{\Gamma_{\text{width}}^{\text{free}}}}$$

Medium modifications of the Delta



$$-\Im(\Sigma_{\Delta}) = C_{QE} (\rho/\rho_0)^{\alpha} + C_{A2} (\rho/\rho_0)^{\beta} + C_{A3} (\rho/\rho_0)^{\gamma}$$

Each contribution corresponds to a different process:

- QE $\implies \Delta N \rightarrow \pi NN$ (still one pion in the final state)
- A2 $\implies \Delta N \rightarrow NN$ (no pions in the final state)
- A3 $\implies \Delta NN \rightarrow NNN$ (no pions in the final state)

We modify the free Delta decay constant to take into account the E-dependent medium modification of the Delta-width

$$\Gamma_{\Delta\pi N}^{\alpha} = \frac{f_{\pi N\Delta} P_{\pi}^{\alpha}}{m_{\pi}}$$

$$f_{\Delta\pi N}^{\text{in-medium}}(W) = f_{\Delta\pi N} \sqrt{\frac{\Gamma_{\text{Pauli}} + 2C_{QE} (\rho/\rho_0)^{\alpha}}{\Gamma_{\text{width}}^{\text{free}}}}$$

References: [*] E. Oset and L. L. Salcedo, Nucl. Phys. A 468, 631 (1987).

Interferences

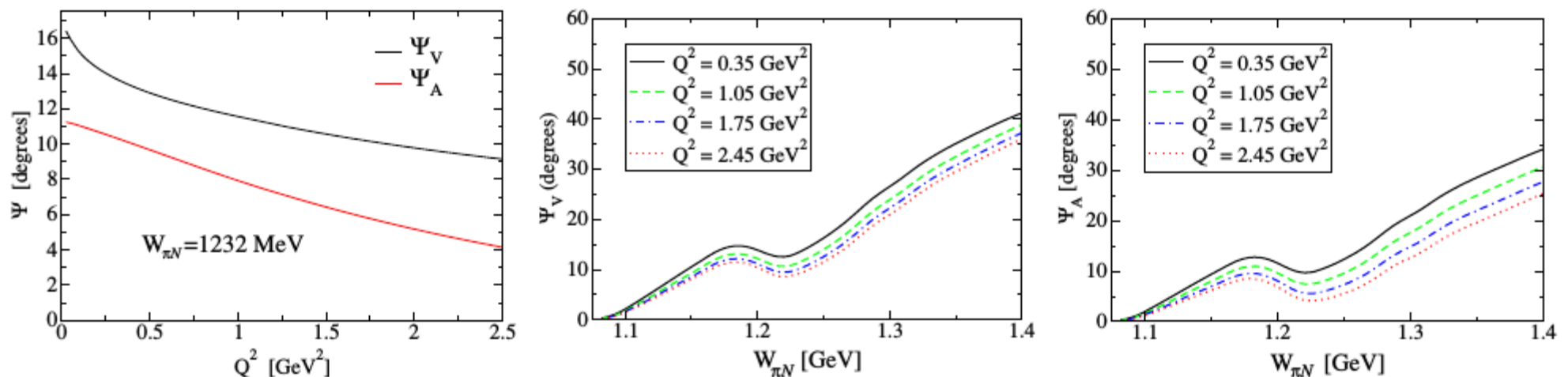
$$J^\nu = \langle J_{\Delta P}^\nu \rangle + \langle J_{C\Delta P}^\nu \rangle + \langle J_{CT,V}^\nu \rangle + \langle J_{CT,A}^\nu \rangle + \langle J_{NP}^\nu \rangle + \langle J_{CNP}^\nu \rangle + \langle J_{PF}^\nu \rangle + \langle J_{PP}^\nu \rangle$$

PHYSICAL REVIEW D **93**, 014016 (2016)

Watson's theorem and the $N\Delta(1232)$ axial transition

L. Alvarez-Ruso,¹ E. Hernández,² J. Nieves,¹ and M. J. Vicente Vacas³

We present a new determination of the $N\Delta$ axial form factors from neutrino induced pion production data. For this purpose, the model of Hernandez *et al.* [Phys. Rev. D 76, 033005 (2007)] is improved by partially restoring unitarity. This is accomplished by imposing Watson's theorem on the dominant vector and axial multipoles. As a consequence, a larger $C_5^A(0)$, in good agreement with the prediction from the off-diagonal Goldberger-Treiman relation, is now obtained.



$$E_m = M_B + M_N - M_A \approx \epsilon_B^* + M_B^0 + M_N - M_A;$$

$$E_S = M_B^0 + M_N - M_A.$$

$$E_m \approx E_S + \epsilon_B^*$$

$$\mathbf{p}_m = \mathbf{p}_A - \mathbf{p}_B = \mathbf{p}_N - \mathbf{q}$$